The Plant Cell, Vol. 23: 1772–1794, May 2011, www.plantcell.org © NRC Canada 2011

The *Arabidopsis* C2H2 Zinc Finger INDETERMINATE DOMAIN1/ENHYDROUS Promotes the Transition to Germination by Regulating Light and Hormonal Signaling during Seed Maturation [W]

J. Allan Feurtado, Daiqing Huang, Leigh Wicki-Stordeur, Laura E. Hemstock, Mireille S. Potentier, Edward W.T. Tsang, and Adrian J. Cutler[1]

Plant Biotechnology Institute, National Research Council Canada, Saskatoon, Saskatchewan, Canada S7N 0W9

Seed development ends with a maturation phase that imparts desiccation tolerance, nutrient reserves, and dormancy degree. Here, we report the functional analysis of an *Arabidopsis thaliana* C2H2 zinc finger protein INDETERMINATE DOMAIN1 (IDD1)/ENHYDROUS (ENY). Ectopic expression of *IDD1*/*ENY* (*2x35S*:*ENY*) disrupted seed development, delaying endosperm depletion and testa senescence, resulting in an abbreviated maturation program. Consequently, mature *2x35S*:*ENY* seeds had increased endosperm-specific fatty acids, starch retention, and defective mucilage extrusion. Using *RAB18* promoter *ENY* lines (*RAB18*:*ENY*) to confine expression to maturation, when native *ENY* expression increased and peaked, resulted in mature seed with lower abscisic acid (ABA) content and decreased germination sensitivity to applied ABA. Furthermore, results of far-red and red light treatments of *2x35S*:*ENY* and *RAB18*:*ENY* germinating seeds, and of artificial microRNA knockdown lines, suggest that *ENY* acts to promote germination. After using *RAB18*:*ENY* seedlings to induce *ENY* during ABA application, key genes in gibberellin (GA) metabolism and signaling were differentially regulated in a manner suggesting negative feedback regulation. Furthermore, GA treatment resulted in a skotomorphogenic-like phenotype in light-grown *2x35S*:*ENY* and *RAB18*:*ENY* seedlings. The physical interaction of ENY with DELLAs and an *ENY*-triggered accumulation of *DELLA* transcripts during maturation support the conclusion that *ENY* mediates GA effects to balance ABA-promoted maturation during late seed development.

INTRODUCTION

The presence of desiccated seeds as reproductive bodies in higher-plant lineages has introduced a maturation phase that imparts stress tolerance upon the seed and provides a mechanism for propagation through both time and space (Bewley and Black, 1994). Temporally, the progression from body plan establishment to resumption of seedling growth involves three phase transitions (Feurtado and Kermode, 2007). One exists in the transition from a mature differentiated embryo to a mature desiccated embryo (eventually surrounded by developed accessory structures, such as the seed coat and endosperm); this encompasses both reserve accumulation and desiccation as the seed becomes a mobile heterotrophic entity. A second occurs as seed dormancy is terminated and germinative processes begin, culminating with the protrusion of the radicle (visible germination). A third transition occurs during seedling growth when light becomes a trigger for photomorphogenesis and an autotrophic existence resumes. However, these are not distinct phase changes and arise during a gradual series of events that occur through development. For example, as Angelovici et al. (2010) note, some of the transcriptional and metabolic changes associated with germination have already commenced during seed desiccation.

The hormone abscisic acid (ABA) promotes seed maturation events, such as the deposition of nutrient reserves, desiccation tolerance, and induction of dormancy (Feurtado and Kermode, 2007; Holdsworth et al., 2008). ABA is an absolute prerequisite for proper progression through maturation as demonstrated by immunomodulation of ABA in tobacco (*Nicotiana tabacum*) and maize (*Zea mays*) *viviparous* mutants (Phillips et al., 1997; White et al., 2000). Although such direct evidence is lacking in *Arabidopsis thaliana*, it is clear that a high ratio of ABA to gibberellin (GA) is an important determinant of maturation and dormancy (Karssen et al., 1983; Debeaujon and Koornneef, 2000; Okamoto et al., 2010). The role of GA during seed development is less obvious. Ectopic expression of a pea (*Pisum sativum*) *GA 2-oxidase* in *Arabidopsis* resulted in both early and late aborted seed (Singh et al., 2002), suggesting a minimal GA content is essential for normal seed development. However, uncovering the full extent of GA function during seed development is not a simple task. The requirement for GA in flower development and pollination, and conceivably embryogenesis, makes identifying what role GA plays during seed maturation, if any, challenging.

In *Arabidopsis*, four major regulators of seed maturation have been characterized: *FUSCA3* (*FUS3*), *ABSCISIC ACID INSENSITIVE3* (*ABI3*), *LEAFY COTYLEDON1* (*LEC1*), and *LEC2* (Nambara

[1] Address correspondence to adrian.cutler@nrc-cnrc.gc.ca.
The author responsible for distribution of materials integral to the findings presented in this article in accordance with the policy described in the Instructions for Authors (www.plantcell.org) is: Adrian J. Cutler (adrian.cutler@nrc-cnrc.gc.ca).
[W] Online version contains Web-only data.
www.plantcell.org/cgi/doi/10.1105/tpc.111.085134

et al., 1992; Luerssen et al., 1998; Lotan et al., 1998; Stone et al., 2001). Mutants of *abi3*, *fus3*, *lec1*, and *lec2* are all severely affected in many aspects of maturation; phenotypes include intolerance to desiccation (*abi3*, *fus3*, and *lec1*), reduced storage protein synthesis (all four mutants), anthocyanin accumulation (*fus3* and *lec1*), chlorophyll degradation (*abi3*), cotyledon misidentity (*fus3*, *lec1*, and *lec2*), and reduced seed dormancy (all four) (Holdsworth et al., 2008). Additional studies have further defined the intricate network relationships that these major regulators form, including redundant and hierarchical regulation (Kagaya et al., 2005; To et al., 2006). *LEC2* and *FUS3* also modulate ABA and GA metabolism (Curaba et al., 2004; Gazzarrini et al., 2004).

Germination in *Arabidopsis*, as with many species, is stimulated by cues such as light, cold, nitrate, and the process of afterripening (Finkelstein et al., 2008). Light stimulation of germination is chiefly triggered through the red (R) and far-red (FR) light-perceiving PHYTOCHROME proteins PHYA and PHYB (Reed et al., 1994). Major regulators of PHY action include PHYTOCHROME-INTERACTING FACTOR (PIF; or PIF3-like [PIL]) proteins whose role is to negatively regulate PHY action (and vice versa) (Shin et al., 2009). During germination, *PIL5* is a key negative regulator of the PHY-mediated promotion of germination (Oh et al., 2004). In addition to indirectly regulating many key pathways involved in germination, PIL5 has been shown to directly regulate such genes as the GA-restraining DELLAs, *REPRESSOR OF GA1-3* (*RGA*), and *GIBBERELLIC ACID INSENSITIVE* (*GAI*), *ABI3*, *ABI5*, GA receptor *GIBBERELLIN INSENSITIVE DWARF1A* (*GID1A*), and *PHYA* and *PHYB* (Oh et al., 2007, 2009). The CCCH zinc finger *SOMNUS* is also directly regulated by PIL5 and has been shown to upregulate GA catabolism and ABA synthesis while downregulating GA biosynthesis and ABA catabolism (Kim et al., 2008). A key process that occurs during the transition to germination, seemingly irrespective of how dormancy is broken, is an increase in the ratio of GA to ABA, through increased GA synthesis and ABA catabolism and activation or derepression of downstream GA signaling (Finkelstein et al., 2008).

The current GA signaling pathway is fairly straightforward. Key regulators include the GID1 GA receptors, the DELLA repressors, SLEEPY1 (SLY1) and SNEEZY F-box proteins, and the *O*-linked *N*-acetylglucosamine transferase (GlcNAc) SPINDLY (SPY) (Peng et al., 1997; Silverstone et al., 1998, 2007; McGinnis et al., 2003; Nakajima et al., 2006; Ariizumi et al., 2011). In the absence of GA, the nuclear-localized DELLA proteins are growth repressing. To upregulate the GA response, bioactive GAs bind to a GID1 receptor (GID1A, B, or C in *Arabidopsis*), promoting its interaction with a DELLA protein. The GA-GID1-DELLA complex shows greater affinity toward SLY1, and DELLA is subsequently degraded by the 26S proteasome pathway (Griffiths et al., 2006; Willige et al., 2007). SPY, a negative regulator of GA signaling, may participate in this regulatory cascade by increasing DELLA activity through GlcNAc modification (Silverstone et al., 2007). In *Arabidopsis*, there are five DELLA proteins, RGA, GAI, RGA-LIKE1 (RGL1), RGL2, and RGL3, which show distinct but overlapping functionality (Sun, 2008). The molecular mechanism of DELLA action is poorly understood; however, two groups have made a major breakthrough regarding DELLA participation in light-regulated hypocotyl elongation. de Lucas et al. (2008) and Feng et al. (2008) demonstrated that the DELLA proteins interact with the DNA binding domain of PIFs (PIF3 and PIF4), thus blocking PIF function and rendering them unable to participate in the promotion of hypocotyl elongation and other skotomorphogenic (dark-growth) traits. Further information regarding DELLA functionality has come from recent articles identifying new protein interactors. These include a DELLA interaction with SCARECROW-LIKE3 (SCL3) and ALCATRAZ (ALC) in a GA regulatory context and the JASMONIC ACID ZIM-DOMAIN (JAZ) proteins, which are key repressors of JA signaling (Arnaud et al., 2010; Hou et al., 2010; Zhang et al., 2011).

In this article, we characterize AT5G66730, a C2H2 zinc finger of unknown function that belongs to the *INDETERMINATE DOMAIN* (*IDD*) gene family, comprising 16 members in *Arabidopsis* (Colasanti et al., 2006). The founding member of the *IDD* family is the maize *INDETERMINATE1* gene, which is involved in floral initiation (Colasanti et al., 1998). Annotated as *Arabidopsis IDD1* by Colasanti et al. (2006), we named AT5G66730 as *ENHYDROUS* (*ENY*), meaning water within, because of the increased water content present during seed development in 2x35S ectopic misexpression (*ENY-ME*) lines. We demonstrate a role for IDD1/ENY in the repression of select maturation traits during seed development and subsequent promotion of PHY- and GA-mediated germination. We also show a direct interaction of IDD1/ENY with the growth-restraining DELLA proteins to substantiate IDD1/ENY as a component in the molecular network of light and hormonal signaling during seed maturation.

RESULTS

ENY mRNA Levels Increase during Seed Maturation

Initial interest in *IDD1*/*ENY* arose from a study linking *IDD1*/*ENY* to secondary seed dormancy in canola (*Brassica napus*) (Fei et al., 2007). Further analysis of various published microarray data sets revealed expression of *ENY* was also associated with dormancy in seeds of the *Arabidopsis* ecotypes Landsberg *erecta* and Cape Verde Islands (Cadman et al., 2006; Carrera et al., 2007). AtGenExpress Development and Hormone microarray data sets also reveal that expression of *ENY* in the *Arabidopsis* life cycle is highest during seed development (Schmid et al., 2005; Goda et al., 2008).

To quantitate *ENY* expression during seed development, particularly during maturation, *ENY* transcript abundance was measured using quantitative RT-PCR (qRT-PCR) in Columbia wild-type seed from 6 d postanthesis (DPA) to 18 DPA and also in mature harvested seed. Consistent with previously published microarray results, *ENY* increased in expression (>50-fold) over the course of seed development (Figure 1A). In addition to Columbia wild type, *ENY* expression was also monitored in transgenic lines modulating *ENY* expression. These were 2x35S ectopic misexpression (*ENY-ME*), *RAB18* promoter-driven *ENY* (*RAB18*:*ENY*), and a *RAB18* promoter-driven artificial microRNA (amiRNA) line (*RAB18*:*ENYami*) that targets *ENY* for downregulation (greater detail on each transgenic line is discussed in subsequent sections). Consistent with the constitutive nature of

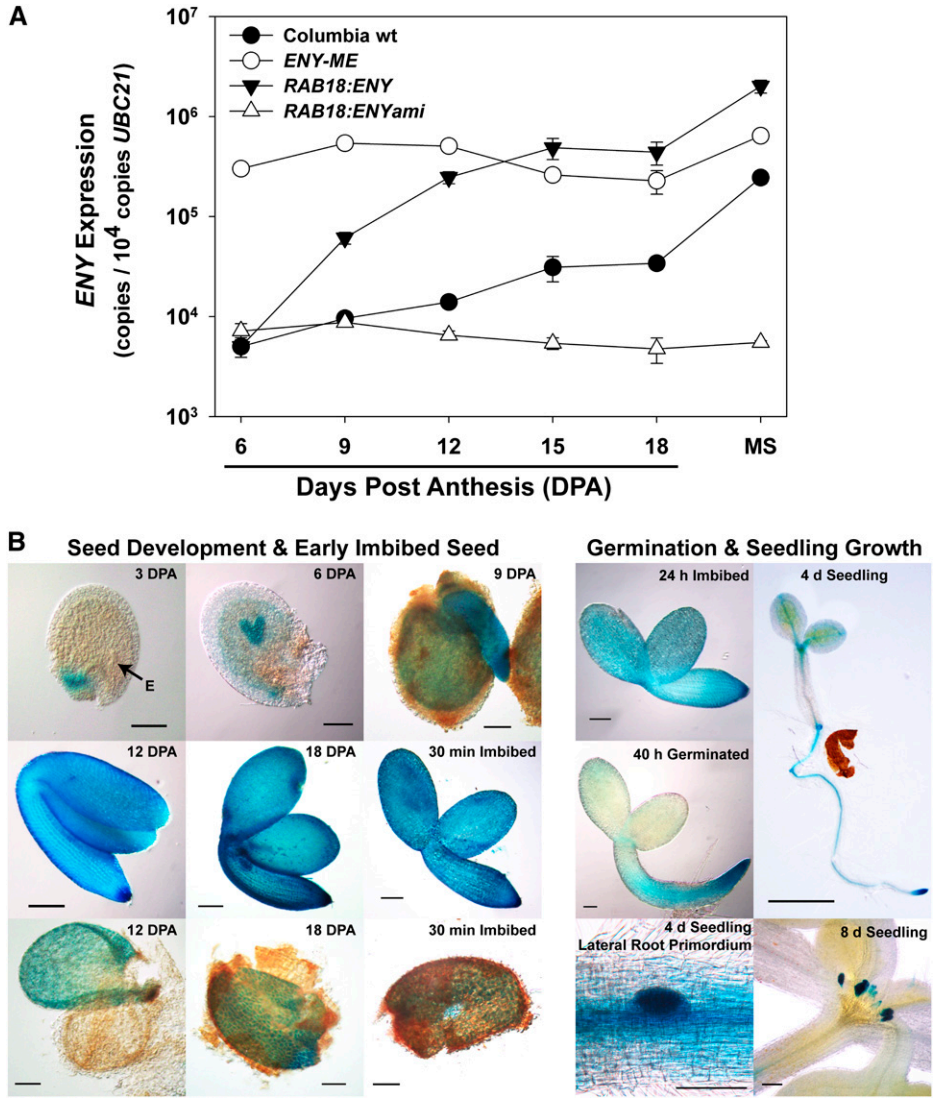

Figure 1. Expression of *ENY* Increased during Seed Maturation.

(A) Expression of *ENY* as assessed by qRT-PCR in Columbia wild type (wt) and various *ENY* transgenic lines, including 2x35S ectopic misexpression (*ENY-ME* line 3), *RAB18* promoter-driven *ENY* (*RAB18*:*ENY* line 13), and a *RAB18* promoter-driven amiRNA line (*RAB18*:*ENYami* line 24). *ENY* expression was normalized to 10^4 copies of *UBC21*. Error bars represent the SE of two biological replicates.

(B) GUS activity driven by a 3-kb upstream promoter sequence of *ENY*. E marks the location of the embryo at 3 DPA. Following fixation in 20% acetone, embryos from later stages were removed from the testa/endosperm to facilitate staining. Bar = 100 μm, except for 4-d-old seedling bar, which represents 1 mm.

the 35S promoter, *ENY-ME* displayed a relatively consistent high abundance of *ENY* transcripts throughout development. The 2x35S promoter produced 60 times more *ENY* transcripts than the native wild-type gene at 6 DPA, but the difference in expression was only 2-fold in mature harvested seed due to the increase in expression of the native gene. In *RAB18*:*ENY*, expression of *ENY* was identical to the wild type at 6 DPA. However, as the *RAB18* promoter was activated, *ENY* expression increased in parallel with the native gene but at levels 6- to 17-fold higher. Expression from *RAB18*:*ENY* was comparable to that produced by *2X35S*:*ENY* at 12 DPA but was higher during later time points. *ENY* transcript abundance in the *RAB18* promoter-driven amiRNA genotype was identical with the native gene and *RAB18*:*ENY* at 6 and 9 DPA but gently decreased at later time points. At the harvested seed stage, *ENY* was 40-fold down-regulated and was almost two orders of magnitude lower than in the wild type (Figure 1A).

To spatially localize *ENY* expression, we monitored activity of β-glucuronidase (GUS) driven by the *ENY* promoter (Figure 1B). At 3 DPA, GUS activity was observed in the chalazal endosperm region. By 6 DPA, activity was present in the endosperm and embryo. GUS staining continued to be apparent in the

endosperm and embryo throughout seed development and continued in the early imbibed seed. Activity decreased during germination, and in the fully germinated seed, GUS staining was strongest in the root tip and absent from the cotyledons. In 4-d-old seedlings, GUS was restricted to the vasculature of the cotyledons, the shoot apical meristem region, and the root. The darkest staining was observed in the root tip and in emerging lateral roots. By 8 d, activity in the shoot was restricted to newly emerged leaves (Figure 1B).

Ectopic Misexpression of *ENY* Delays Seed Maturation Events

To functionally characterize *ENY*, we generated 2x35S misexpression lines using the open reading frame (ORF) of *ENY* (AT5G66730) (hence named *ENY-ME*) and obtained publicly available T-DNA insertion lines. However, no reduction in expression of *ENY* in mature rosette leaves of homozygous T-DNA lines was observed using qRT-PCR. Thus, initial analyses were focused on *ENY-ME* lines. After seed imbibition and staining with ruthenium red, we observed defective mucilage extrusion in 42% of T1 transgenic lines (see Supplemental Figures 1 and 2 online). Subsequently, analyses of two independent homozygous lines (3 and 19) in the T3 and T4 generations revealed that *ENY* misexpression perturbed many developmental processes, including fertility, seed development, germination, and seedling establishment (see Supplemental Figures 3 and 4 online). However, because of the association of *ENY* expression with seed dormancy, we focused on the role of *ENY* in seed development and germination.

A significant delay in *ENY-ME* seed development was observed, especially with respect to senescence of the seed coat and depletion of the endosperm (Figures 2 and 3; see Supplemental Figure 5 online). As a consequence, *ENY-ME* seeds were bigger than those of Columbia wild type due to an enlarged endosperm. The increase in the size of the endosperm appears to be due to an increase in cell number. For example, in the sections depicted in Figure 3, at 6 DPA there are 185 cells in the *ENY-ME* line versus 160 in Columbia wild type. The *ENY-ME* seed coats contained the traditional five cell layers, as in Columbia wild type (Haughn and Chaudhury, 2005). An enlarged endosperm is especially evident at 8 DPA when in the wild type there were only three to five cell layers of endosperm remaining and the embryo was constrained into the folded U-shape. In *ENY-ME*, a large amount of endosperm remained and the embryo was not U-shaped (Figures 2A and 3). The seed coat of *ENY-ME* at 8 DPA was similar to Columbia wild type, except that the epidermal cell layer appeared larger; however, this may be partly due to artificial swelling of the mucilage during aqueous fixation. At 10 DPA, embryo sizes were similar but the endosperm in *ENY-ME* lines retained three to five cell layers, while in wild-type endosperm, development was mostly complete and had shrunk to one to two cell layers with a distinct endosperm aleurone layer appearing. The seed coat at 10 DPA was thicker in *ENY-ME* lines; this appeared to be due to the increased size of cells underlying the epidermal layer such as the endothelium cells (Figure 3). By 15 DPA, wild-type seed coat development was mostly complete; however, *ENY-ME* seed coats were still translucent with limited

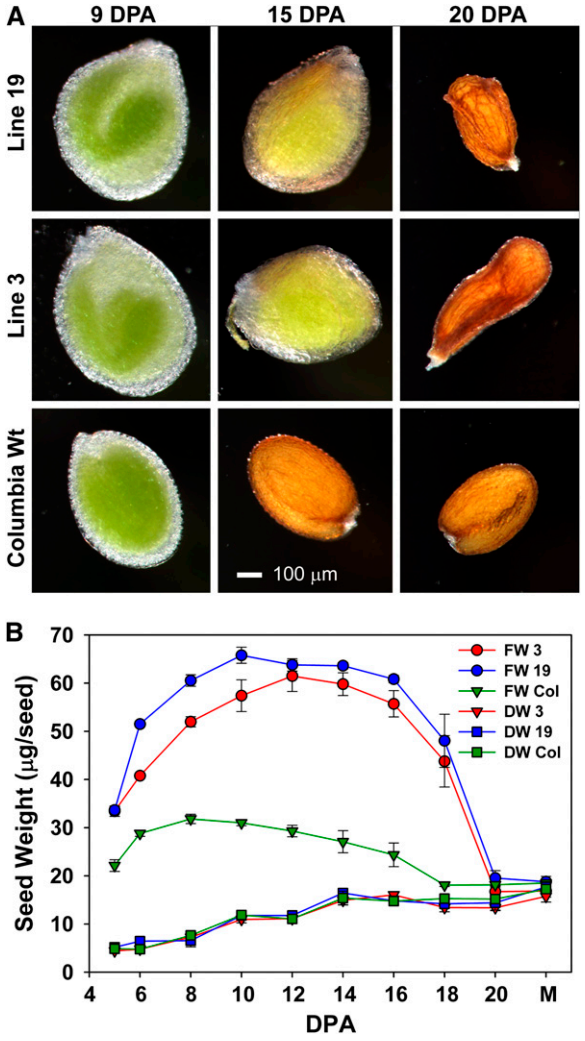

Figure 2. Progression of Seed Development Is Delayed in *ENY* Misexpressing Lines.

(A) At 9 DPA, seeds of *ENY-ME* lines were larger than those of Columbia wild type (Wt), especially with respect to the endosperm. By 15 DPA, development was almost complete in seeds of Columbia wild type; however, in *ENY-ME* lines, the seed coat was just beginning to pigment and had not senesced. At 20 DPA, mature dry seeds of *ENY-ME* lines desiccated abruptly, and as a consequence, select seeds appeared to have a shriveled seed coat or embryos that were not in the characteristic U-shape.

(B) The visible increases in seed size presented in **(A)**, compared with Columbia (Col) wild type, were manifest in the fresh weight (FW) of *ENY-ME* lines. However, the dry weights (DE) of *ENY-ME* lines were similar to those of the wild type. Error bars represent the SE of a minimum of three replicates of 20 to 30 seeds. Mature harvested seed is denoted as M.

pigmentation (Figure 2A). The fresh weight (water content) of *ENY-ME* was increased, but on a dry weight basis, *ENY-ME* seeds were not significantly different from Columbia wild type (Figure 2B). Unlike Columbia wild type, the desiccation of *ENY-ME* seeds was abrupt; most of the fresh weight was lost between 18 and 20 DPA (Figure 2B). By the end of seed maturation, mature *ENY-ME*

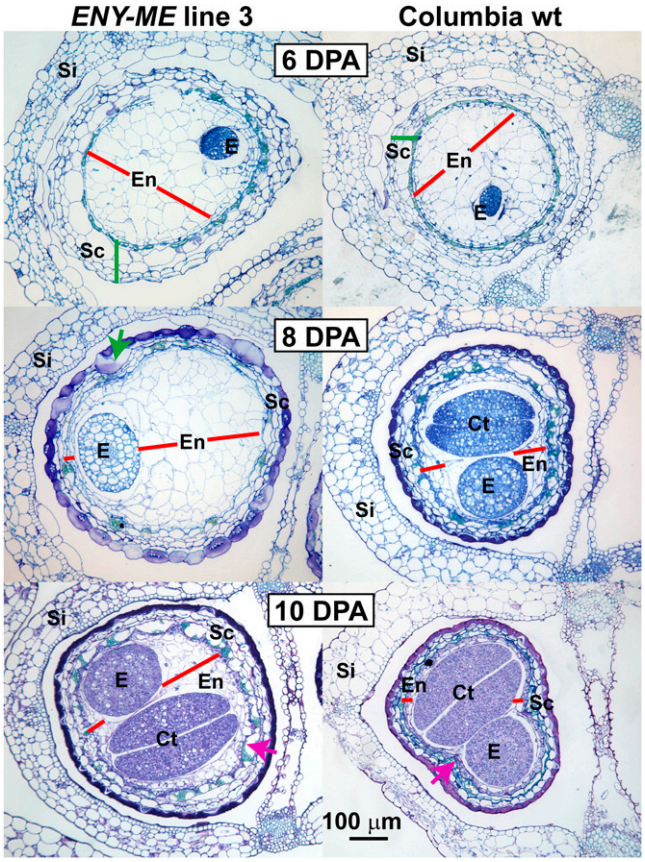

Figure 3. Delayed Endosperm Depletion during *ENY* Ectopic Misexpression.

The area of *ENY-ME* seeds, as measured by ImageJ, was consistently 1.5-fold larger than Columbia wild type (wt) (0.27 versus 0.18 mm^2, 0.30 versus 0.20 mm^2, and 0.26 versus 0.17 mm^2 at 6, 8, and 10 DPA, respectively). The increase in area was due to an increase in endosperm and seed coat size. At 6 DPA, cell numbers in the endosperm of *ENY-ME* totaled 185, while Columbia wild type totaled 160. At 8 DPA, increased *ENY-ME* endosperm size meant that the embryo was no longer constrained in the prototypical U-shape. At 10 DPA, significant endosperm still remained to be absorbed in *ENY-ME*, a process mostly complete in Columbia wild type. The seed coat was also noticeably thicker at 10 DPA; pink arrows represent the comparison between endothelium cells of *ENY-ME* and Columbia wild type. Ct, cotyledons; E, embryo axis; En, endosperm; Sc, seed coat; Si, silique. Green arrow at 8 DPA represents a cell where mucilage has artificially expanded during aqueous fixation.

embryos were of similar size and had lost chlorophyll but were more translucent than their wild-type counterparts (see Supplemental Figure 6 online).

The apparent delay in *ENY-ME* seed maturation prompted us to measure seed storage compounds in the mature seed. Total protein extracted from *ENY-ME* lines and Columbia wild-type seed grown at the same time showed an average decrease of ~21 and 27% in lines 3 and 19, respectively (see Supplemental Figure 7A online). Consistent with the increased endosperm size, several endosperm-specific fatty acids (Penfield et al., 2004) were increased in mature seeds of *ENY-ME* lines (see Supplemental Figure 7B online). Sugars, including Suc, Glc, raffinose, and stachyose, were also increased in *ENY-ME* line 19. A significant amount of starch was present in mature seeds of *ENY-ME* line 19 but not in mature Columbia wild-type seed (see Supplemental Figure 7C online). Mature Columbia seed does not usually contain starch since it accumulates only transiently in *Arabidopsis* seed development (Focks and Benning, 1998).

To identify changes in gene expression associated with *ENY* action, we performed a two-color microarray analysis comparing *ENY-ME* line 19 to Columbia wild type at 5 DPA, 10 DPA, and mature seed (see Supplemental Data Set 1 online). Differentially expressed gene (DEG) lists, containing both up- and downregulated genes, were identified using a false discovery rate (FDR) of 5% using a modified *t* test in Significance Analysis of Microarrays (SAM) and 1.5-fold change in expression (Tusher et al., 2001). Consistent with phenotypic observations and measurement of storage compounds, transcript profiles of *ENY-ME* were at a more juvenile stage than those of the wild type. For example, at 10 DPA, Gene Ontology (GO) terms overrepresented in the downregulated genes (at $P \leq 0.001$) included alkaloid metabolism, flavonoid and lignin biosynthesis, and response to water deprivation (see Supplemental Data Set 1 online). Reduced expression of genes associated with these processes is consistent with the observed delays in seed coat development and delayed desiccation in *ENY-ME* seeds compared with Columbia wild type. However, in mature *ENY-ME* seeds, several GO terms overrepresented in the upregulated genes suggest *ENY-ME* seeds rapidly advanced through the desiccation process: response to ABA, desiccation, water deprivation, cold, salinity, galactose metabolism, and Pro biosynthesis. Thus, the overall effect of *ENY* misexpression is to delay seed maturation events, especially with respect to seed coat senescence and endosperm assimilation.

Induction of *ENY* in Seedlings Shifts Expression of GA Pathway Genes

The significant developmental perturbations in *ENY-ME* lines during seed development meant that direct comparisons of tissues of the same age could not reveal the precise effects of *ENY*. Differences in patterns of gene expression could reflect shifts in timing of development rather than the direct effects of *ENY* on gene expression. Therefore, it was decided to direct expression specifically to seed maturation using the *RAB18* promoter. We anticipated that the *RAB18* promoter would direct expression in a similar temporal/developmental pattern as *ENY* but at a higher level (as confirmed in Figure 1A). *RAB18* is also spatially localized throughout the embryo and endosperm in dry seeds (Nylander et al., 2001); this parallels *ENY* promoter activity as shown by GUS staining (Figure 1B). Therefore, *RAB18*:*ENY* transgenic lines should reveal the true function of *ENY* during seed maturation more precisely than the 2x35S lines. Since the *RAB18* promoter is not expressed during early seed development, some of the confounding effects due to delayed entrance into seed maturation would be avoided. Accordingly, the seed phenotypes described for the *ENY-ME* plants described above (e.g., delayed seed coat senescence and mucilage defect) were absent in the *RAB18*:*ENY* plants (see Supplemental Figure 8 online). This suggests that the effects in *ENY-ME* lines are initiated early in seed development,

before *ENY* is normally expressed at a high level. However, as described below, other *ENY-ME* phenotypes were recapitulated in *RAB18*:*ENY*.

Having created transgenic *RAB18*:*ENY* lines to investigate high level expression effects during late seed development, we subsequently used these lines in an inducible system to determine the short-term effect of increased *ENY* expression on the *Arabidopsis* transcriptome. To accomplish this, *RAB18*:*ENY* seedlings were treated with 10 μM (+)-ABA to induce *ENY* (Ghassemian et al., 2000). After obtaining three independent T2 *RAB18*:*ENY* lines, 5-d-old seedlings were selected to perform the inductions, since the seedlings were easy to manipulate and expression of the *RAB18* promoter under control conditions was minimal. Initial testing, using qRT-PCR expression analysis, showed that maximal expression of *ENY* occurred 3 h after transfer of the seedlings to (+)-ABA (see Supplemental Figure 9A online). It is also important to note that expression of *ENY* was not affected by ABA treatment in Columbia wild type (see Supplemental Figure 9B online). Nonetheless, knowing that the presence of ABA would alter seedling physiology, a transgenic *ENY* line was always compared with like-treated Columbia wild type (i.e., 3 h ABA-treated *RAB18*:*ENY* compared with 3 h ABA-treated Columbia wild type).

Two representative *RAB18*:*ENY* transgenic lines (2 and 16) displayed increases in *ENY* expression of 5-fold at time 0 and 73- and 57-fold after 3 h (+)-ABA, respectively (see Supplemental Figure 9A online). We compared *RAB18*:*ENY* to Columbia wild type at both time 0 (No ABA) and after 3 h with ABA (3 h ABA) (*RAB18*:*ENY* results were averaged between lines 2 and 16). There were only 22 DEGs in the No ABA comparison (see Supplemental Data Set 2 online). Notable in this list was downregulation of the GA biosynthesis gene *GA 20-oxidase 2* (*GA20ox2*) in *RAB18*:*ENY* lines (see Supplemental Data Set 2 online). After treatment with ABA and subsequent *ENY* induction (3 h ABA), there were 221 DEGs (43 upregulated/178 downregulated). Several additional GA metabolism or signaling genes were present in the 3-h ABA DEG list (significantly changed ≥1.5-fold). The catabolic genes *GA2ox6* and *GA2ox1* were upregulated, and the biosynthesis genes *GA20ox2* and *GA3ox1*, the GA receptor *GID1B*, transcriptional regulator *SCL3*, and F-box *SLY1* were downregulated (Figure 4A; see Supplemental Data Set 2 and Supplemental Figure 10 online).

We used qRT-PCR to further investigate the impact of *ENY* expression on GA metabolism and signaling. In this experiment, in addition to inducing *ENY* with 3 h (+)-ABA treatment, either 10 μM GA_3 or 1 μM paclobutrazol (PAC; an inhibitor of GA biosynthesis) was included (see Supplemental Figure 9C online). The induction of *ENY* was similar in the various treatments with the exception of *RAB18*:*ENY* line 13 under ABA/GA (195-fold upregulated in ABA/GA versus 235 in the other two treatments, ABA or ABA/PAC) (see Supplemental Figure 9C online). As in the microarray results, increased expression of *ENY* resulted in upregulation of negative components of GA metabolism or signaling and downregulation of positive components of GA metabolism or signaling (Figure 4B). The largest changes in expression were observed under the ABA/GA treatment in the highest-expressing *RAB18*:*ENY* line, line 13. For example, comparing line 13 to Columbia wild type after 3 h ABA treatment, major changes in *GA20ox2*, *GA3ox1*, and *GA2ox1* expression were observed (fold change of −4.0, −3.0, and 8.2, respectively). Under ABA/GA treatment, the expression of the aforementioned genes changed, −15.3-, −17.6-, and 15.7-fold, respectively. The effect of PAC combined with ABA produced expression changes that were close to those observed for ABA alone (Figure 4B). It was expected that PAC application would reduce the negative transcriptional impacts of *ENY* on GA homeostasis. However, this may have been masked due to the application of ABA or simply the presence of *ENY* itself. Nevertheless, these results associated *ENY* with GA metabolism and signaling. The next step in assigning a function to *ENY* was to investigate its possible association with other components of the GA pathway.

ENY Is a Negative Regulator of Photomorphogenesis in the Presence of GA

Following germination, *Arabidopsis* seedlings exposed to light undergo photomorphogenesis, which is characterized by reduced hypocotyl elongation, cotyledon opening and expansion, production of chlorophyll, and resumption of photosynthesis. In the dark, skotomorphogenic (or etiolated) seedlings have long hypocotyls, closed cotyledons in an apical hook, and contain etioplasts instead of chloroplasts. Etiolated growth is driven by GA and reducing endogenous GA levels partially derepresses photomorphogenesis in the dark (Alabadí et al., 2004). Thus, because results from the induction experiments seemed to associate ENY with GA homeostasis, we investigated the effect of *ENY* on seedling growth with and without addition of exogenous GA.

After 7 d growth in white light, the hypocotyl length and cotyledon angle of *ENY-ME* lines were similar to Columbia wild type when grown on control plates with 0.5 Murashige and Skoog (MS) salts (Figure 5). However, when grown in the light with 10 μM GA_3, *ENY-ME* lines displayed hypersensitive effects. *ENY-ME* hypocotyl lengths were more than double the length of Columbia wild type (Figure 5A). In addition, cotyledon angles of *ENY-ME* seedlings grown in the presence of GA were smaller than their wild-type counterparts (Figure 5A). The hypocotyl effect was increased slightly when 1% Suc was added to the medium (see Supplemental Figure 11 online). These phenotypes, together with the presence of shorter roots and chlorotic, yellow cotyledons and leaves (Figure 5B; see Supplemental Figure 11B online), resemble dark-growth (skotomorphogenic) phenotypes. However, unlike etiolated seedlings, cotyledon expansion and activation of the shoot apical meristem were not appreciably affected. We classified the skotomorphogenic-like phenotype of light-grown *ENY-ME* lines as GA-hypersensitive (1) because of the intimate association of GA with etiolated growth (Alabadí et al., 2004) and (2) because the phenotype was associated with exogenous GA application. A similar GA-hypersensitive phenotype was also observed in *RAB18*:*ENY* seedlings when grown under 10 μM GA_3 and 0.45 μM (+)-ABA to induce *ENY*, but only with respect to increased hypocotyl elongation (see Supplemental Figure 12 online). A mild phenotype was not unexpected, however, as *ENY* expression would not be sustained under the *RAB18* promoter, partly because ABA was applied at a low concentration and would be rapidly metabolized (Huang et al., 2007).

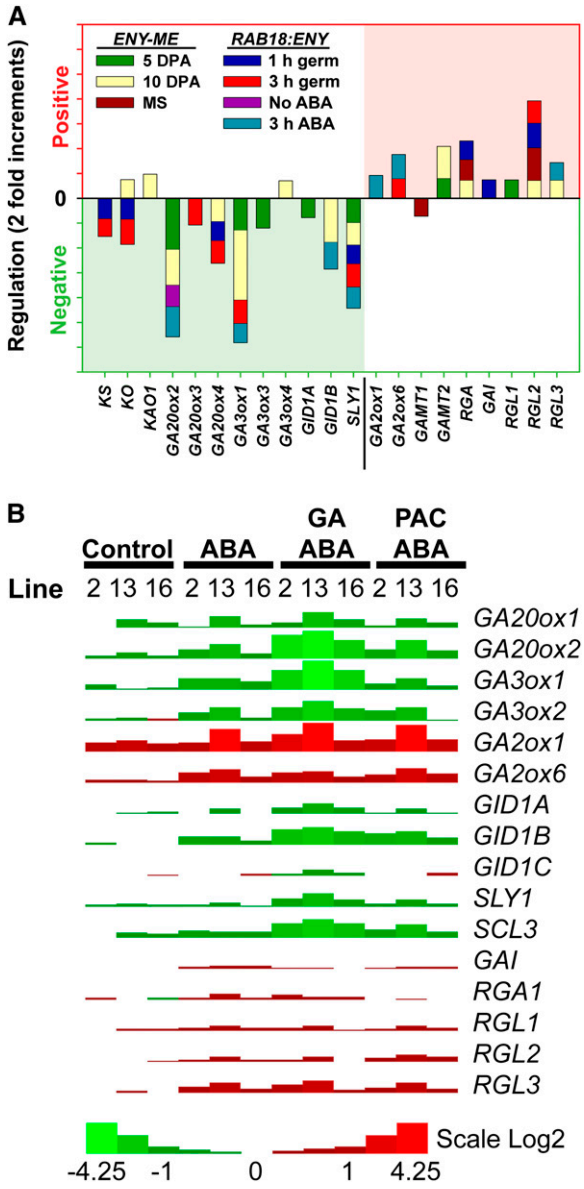

Figure 4. *ENY* Represses Expression of GA Synthesis and Signaling Genes.

(A) Microarray analysis detected altered expression of GA pathway genes in *ENY* transgenic lines. Increased expression of *ENY*, driven by the 2x35S (*ENY-ME*) or *RAB18* promoter, resulted in downregulation of GA synthesis and signaling genes and upregulation of catabolism and *DELLA* regulatory factors. Each colored segment of a complete bar shows the fold change between a given ENY transgenic line and Columbia wild type (FDR 0.05 and fold change > 1.4). MS, mature harvested seed; germ, germination; No ABA, 5-d-old seedlings; 3 h ABA, 5-d-old seedlings treated with ABA for 3 h. Lines used for microarray analyses included *ENY-ME* line 19 for seed development, *RAB18*:*ENY* line 13 for imbibed seed, and *RAB18*:*ENY* lines 2 and 16 for 5-d-old seedlings under ABA treatment.

(B) Expression of GA pathway genes, as assessed by qRT-PCR, was altered by artificially increasing *ENY* expression during ABA treatment with or without added GA or PAC in 5-d-old seedlings of *RAB18*:*ENY* lines (see Supplemental Figure 9C online). *ENY* produced a regulatory action that acted against GA synthesis and signaling. The effect was amplified when GA was added, suggesting *ENY* alters feedback regulation. Relative fold change compared with Columbia wild type is expressed as log2 ratios, and qRT-PCR primers are presented in Supplemental Table 2 online. Biological replication of the experiment was performed through analysis of the three independent *RAB18*:*ENY* transgenic lines. The RNA for Columbia wild type and each transgenic line was pooled from a minimum of 24 5-d-old seedlings grown on three independent agar plates (for each treatment).

ENY Promotes Phytochrome-Mediated Seed Germination

Next, we investigated the effect of *ENY* overexpression during early germination. After confirming that *ENY* was differentially expressed in dry and imbibed seeds of *RAB18*:*ENY* lines (see Supplemental Figure 13A online), we performed microarray analyses comparing *RAB18*:*ENY* line 13 to Columbia wild type after 1 and 3 h in germination conditions under white light (WL) (see Supplemental Data Set 3 online). The comparison yielded 945 DEGs (241 upregulated/704 downregulated) after 1 h seed imbibition and 735 DEGs (229 upregulated/506 downregulated) after 3 h seed imbibition. Consistent with the previous *ENY* induction experiment results, GA biosynthesis and signaling were repressed while GA catabolism and negative regulatory factors were activated (Figure 4A; see Supplemental Data Set 3 online).

In a recent study, Oh et al. (2009) suggested *ENY* is a direct downstream target for regulation by PIL5. Based on this information and our association of *ENY* with the inhibition of photomorphogenesis, we compared the DEGs in our data set, comparing *RAB18*:*ENY* to Columbia wild type after 1 h in germination conditions, with two data sets available online from the Gene Expression Omnibus (GEO) archive (Barrett et al., 2009). The first study, from Oh et al. (2009), compared Columbia wild-type imbibed seed treated with FR and red R light pulses to that treated with a FR light pulse alone (after a subsequent 12 h in the dark), hence named Col-0(D)/Col-0(R). Treatment with an R light pulse stimulates phytochrome-mediated germination of Columbia wild type seeds in the dark. Thus, in the FR/R treatment, the transcriptional profiles would be those of a germination-stimulated nature. A considerable proportion of DEGs in our *RAB18*:*ENY*/Columbia data set overlapped with the Col-0(R)/Col-0(D) DEGs (Figure 6A; see Supplemental Data Set 3 online). For example, 45% of genes downregulated by the presence of *ENY* at 1 h white light were also downregulated by red light after 12 h; whereas 28% were commonly upregulated by both *ENY* and red light. The second experiment, from Leivar et al. (2009), compared the quadruple *pifq* mutant (*pif1 3 4 5*) and Columbia wild type after 5 d of moist chilling, hence named *pifq*(seed)/Col-0(seed). As mentioned, PIFs are negative regulators of phytochrome action, and the *pifq* mutant, because of the lack of the PIL5/PIF1 protein, can germinate in the dark without the need for a R light cue (Shin et al., 2009). Similar to the comparison to R light, substantial overlap occurred between the *RAB18*:*ENY*/Columbia and the *pifq*(seed)/Col-0(seed) comparison (Figure 6A; see Supplemental Data Set 3 online). Here, 36% of the genes downregulated by

the presence of ENY at 1 h in germination conditions were also downregulated by PIF absence, whereas 19% were commonly upregulated by increased ENY presence and PIF absence. Thus, ENY regulated, perhaps indirectly, a high proportion of genes modulated by both red light and PIFs, in the same direction as red light but opposite to the action of PIFs.

After finding substantial overlap between ENY-regulated transcription, red light, and PIFs, we tested the germination response of *ENY* mis- and overexpression lines to both FR and R light. We focused on FR and R light treatment early in the imbibition process since two-thirds of *ENY* transgenic lines were driven by the *RAB18* promoter and expression from this promoter is greatly reduced within the first 5 h of imbibition (see Supplemental Figure 13A online). Because FR and R light were applied during the first 1 to 2 h of imbibition, PHYB, mediating the R light low fluence response, would be expected to be the dominant phytochrome promoting germination at this time (Reed et al., 1994; Shinomura et al., 1994). Following plating of seeds under

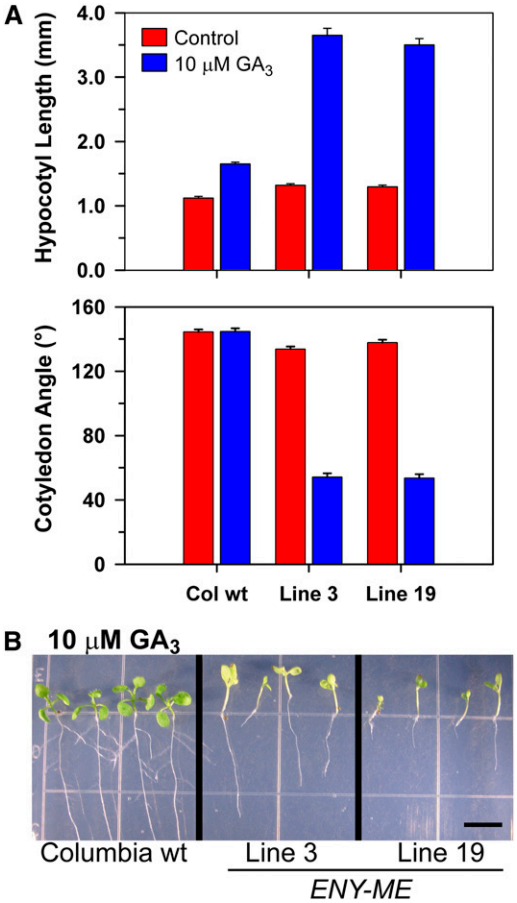

Figure 5. Growth of *ENY* Misexpression Seedlings under GA Treatment Results in a Skotomorphogenic-Like Phenotype.

(A) Hypocotyl length and cotyledon angle of *ENY-ME* and Columbia wild-type (Col wt) 7-d-old seedlings grown with or without GA_3. Error bars represent the SE of at least 50 measured seedlings.
(B) Seedling phenotype under GA treatment of *ENY-ME* seedlings as detailed in **(A)**. Bar = 5 mm.

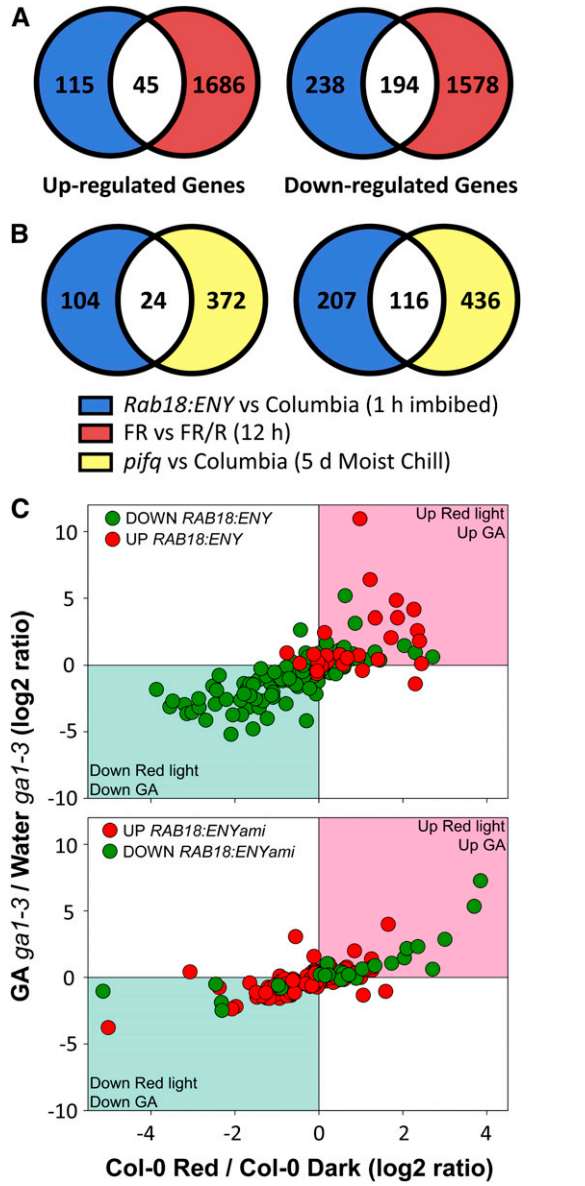

Figure 6. *RAB18 ENY* Array Data Display Similarities to Red Light, the Quadruple *pif* Mutant, and GA-Treated *ga1-3* Data Sets.

(A) Overlap of genes between *RAB18:ENY*/Columbia wild type 1 h imbibed seed array data and the data of Oh et al. (2009) comparing FR light/FR-R light 12 h after the start of seed imbibition.
(B) As in **(A)** but comparison of our data to Leivar et al. (2009) data comparing *pif1 3 4 5* quadruple mutant seed to Columbia wild type seed moist-chilled for 5 d.
(C) Comparison of genes changed ≥2-fold in *RAB18 ENY* knockdown and overexpression 1 h imbibed seed microarray data sets (see Supplemental Data Sets 3 and 4 online) with Oh et al. (2009) data set described in **(A)** and Ogawa et al. (2003) data set. The Ogawa et al. (2003) data set compared *ga1-3* seed treated with GA for 9 h to *ga1-3* treated with water for 9 h.

white light for 1 h, seeds were treated with a pulse of 4 μmol/m^2/s FR for 6 min. Consistent with the observed changes in transcriptional events in *RAB18*:*ENY*, both *ENY-ME* and *RAB18*:*ENY* lines were less sensitive to germination inhibition by FR light (see Supplemental Figure 14 online). To stimulate PHYB-mediated germination after the white light and FR treatment, seeds received 30 μmol/m^2/s R light for 10 min. Here, FR/R light treatment promoted germination to virtually 100% in both *ENY* lines and Columbia wild type (see Supplemental Figure 14 online). Thus, *ENY* alters the behavior of *Arabidopsis* seeds so that they are less dependent on light-triggered cues for germination.

Knockdown of *ENY* in Seeds Supports a Role in Light and Hormonal Signaling

Since no T-DNA insertion lines resulted in differences to *ENY* expression, amiRNA methodology was used to attenuate (knockdown) *ENY* expression (Schwab et al., 2006). As before, for a high level of seed-specific expression during seed maturation, we used the *RAB18* promoter to drive amiRNA expression, and this resulted in a reduction of 96 to 98% in mature T3 homozygous seeds (see Supplemental Figure 13B online).

Because *ENY-ME* and *RAB18*:*ENY* lines displayed altered FR and R light germination, we tested the response of *RAB18*:*amiENY* lines under similar conditions. Opposite to *ENY* overexpression lines, knockdown lines were less sensitive to germination promotion by R light compared with Columbia wild type (see Supplemental Figure 14 online). Since *RAB18*:*amiENY* line 24 showed the greatest phenotypic germination response and largest *ENY* knockdown, we used this line for microarray experiments.

For uniformity with the *RAB18*:*ENY* data sets, we compared *RAB18*:*amiENY* line 24 and Columbia wild type after 1 h in germination conditions under white light. Using the same criteria as in previous experiments, 620 DEGs (392 upregulated and 228 downregulated) were identified in the *RAB18*:*amiENY* to Columbia comparison (see Supplemental Data Set 4 online). Unlike the results of the *RAB18*:*ENY* arrays, few GA synthesis or signaling genes were revealed. In fact, only *GA2ox6* was present within the DEG lists and was downregulated (*GA20ox3* was significantly [1.44-fold] upregulated). However, several factors involved in light and phytochrome signaling networks were altered (see Supplemental Table 1 online). For instance, inhibitors of photomorphogenesis were upregulated, such as *CONSTITUTIVE PHOTOMORPHOGENIC10* (*COP10*)/*FUS9* and *SUPRESSOR OF PHYA 1-LIKE3* (*SPA3*) (Suzuki et al., 2002; Laubinger and Hoecker, 2003). Other factors involved in light signaling that were downregulated in the knockdown line included the downstream PHYA factor *LONG AFTER FAR-RED3* (*LAF3*) and the shade avoidance–related factor *ARABIDOPSIS THALIANA HOMEOBOX PROTEIN2* (*ATHB2*) (*PHYA* itself was significantly [1.33-fold] downregulated) (Steindler et al., 1999; Hare et al., 2003). Another trend in *RAB18*:*ENYami* DEGs was the upregulation or derepression of genes involved in photosynthesis and associated processes. Four subunits of RUBISCO, 14 genes involved in the photosynthetic light reactions, and two enzymes in the photorespiratory pathway were upregulated in *ENY* knockdown seed (see Supplemental Data Set 4 online). The derepression of photosynthetic processes, even after 1 h in germination conditions, is consistent with a role for *ENY* in skotomorphogenic-like signaling.

The expression of the two GA metabolic genes, *GA2ox6* and *GA20ox3*, in the *ENY* knockdown line was opposite to that observed in the *RAB18*:*ENY* overexpression line, further suggesting a consistency in the phenotypes. However, when comparing the entire data sets, only 71 DEGs were oppositely regulated in *RAB18*:*ENY* and *RAB18*:*amiENY* comparisons (see Supplemental Data Set 4 online). Seventeen DEGs were upregulated in *RAB18*:*ENY* and downregulated in *RAB18*:*amiENY*, and 54 were common in the opposite direction (downregulated in *RAB18*:*ENY* and upregulated in *RAB18*:*amiENY*) (see Supplemental Data Set 4 online). A deeper comparison with *ENY RAB18* overexpression and knockdown gene lists revealed that several genes involved in light or hormonal signaling were significantly regulated in the opposite direction (see Supplemental Table 1 online). For instance, in the ABA signaling pathway, the negative regulator *ABI1* was upregulated with *ENY* overexpression and downregulated when *ENY* expression was knocked down. Similarly, *GNC* (for *GATA*, *NITRATE-INDUCIBLE*, *CARBON-METABOLISM INVOLVED*), which was recently identified as a repressor of GA responses (Richter et al., 2010), was upregulated in the *RAB18*:*ENYami* knockdown line and downregulated in the *ENY-ME* and *RAB18*:*ENY* overexpression lines (see Supplemental Data Set 3 and Supplemental Table 1 online).

As a final comparison for the *RAB18*:*ENY* and *RAB18*:*amiENY* data sets, we examined how DEGs in our data sets changed during red light and GA treatment. To accomplish this, we used the Col-0(R)/Col-0(D) data from Oh et al. (2009) mentioned above and an additional GEO microarray data set, from the AtGenExpress consortium, comparing *ga1-3* seed treated with 5 μM GA_4 to *ga1-3* treated with water after 9 h in white light, hence named *ga1-3*(GA)/*ga1-3*(water) (Ogawa et al., 2003; Goda et al., 2008). After creating a virtual GeneSpring experiment with the red light and *ga1-3* data expressed as log2 ratios, we imported *RAB18*:*ENY* and *RAB18*:*amiENY* gene lists and found that DEGs with ≥2-fold change showed the clearest trend. It is evident in Figure 6C that genes upregulated by *ENY* overexpression had a tendency to be upregulated by both red light and GA, while genes downregulated by *ENY* overexpression displayed the opposite trend (Figure 6C). The trend is modest, but still evident and opposite, in the *RAB18*:*ENYami* knockdown line. Genes downregulated by *ENY* knockdown were normally upregulated by red light and/or GA; genes upregulated when *ENY* was knocked down tended to be downregulated by red light and/or GA (Figure 6C). These results are consistent with the premise that ENY acts as a positive regulator of phytochrome and/or GA action.

ENY Antagonizes ABA Accumulation and Response

Having associated *ENY* with phytochrome and GA signaling, attention was shifted to ABA. Antagonism of GA and ABA has been documented from the earliest of studies in *Arabidopsis*; a key example was obtained when the ABA-deficient mutant *aba1* was recovered in a suppressor screen for the GA-deficient *ga1* mutant (Koornneef et al., 1982). To assess response to ABA, we tested the various *ENY* transgenic lines for sensitivity of germination to exogenous ABA. Consistent with the GA-hypersensitive

phenotype of *ENY-ME* seedlings, *ENY-ME* and *RAB18*:*ENY* transgenic lines were less sensitive to the inhibition of germination by applied ABA. Of note, *ENY-ME* lines germinated slower than Columbia wild type on water with or without prior moist chilling (Figure 7A; see Supplemental Figure 15 online); this may be related to the mucilage defect present in *ENY-ME* lines (Arsovski et al., 2009). Despite the delay in germination, the insensitivity of germination to ABA in *ENY-ME* lines was revealed at 1 and 10 μM (+)-ABA (Figure 7A; see Supplemental Figure 16 online). In contrast with the mis- and overexpression lines, *RAB18*:*ENYami* knockdown line 24 was more sensitive to germination inhibition by exogenous ABA (Figure 7A). If the light intensity was lowered from 90 to 40 μmol/m^2/s, line 21 also displayed greater sensitivity to exogenous 0.5 and 1 μM (+)-ABA compared with Columbia wild type (see Supplemental Figure 16 online). Maintaining the consistency of *ENY* as an antagonist to ABA, mature seeds of both *ENY-ME* and *RAB18*:*ENY* lines contained lower amounts of endogenous ABA compared with Columbia wild type (Figure 7B).

ENY Physically Interacts with the DELLA Protein Family

In order to better define the functional context of *ENY*, we performed a yeast two-hybrid protein–protein interaction analysis. To that end, a commercially available *Arabidopsis* library from Clontech was screened for ENY interactors. The premade Clontech library was constructed with normalized cDNA from 11 different *Arabidopsis* tissues (see Methods). Initially, the ORF for *ENY* was cloned into the pGBKT7 vector. However, expression of ENY with a 706-bp fragment of the *Saccharomyces cerevisiae ADH1* promoter led to activation of all transcriptional reporters/selectable markers (often termed autoactivation). To avoid this problem, we expressed ENY under a weaker promoter; the vector pGBT9, containing a 396-bp *ADH1* promoter, was used for this purpose. Using pGBT9, autoactivation was reduced to minimal levels on the highest stringency plates (Figure 8A).

Following screening of >11 million yeast library clones through diploid mating, ~300 blue colonies of potential ENY interactors were recovered. After sequencing 90 of the potential ENY interactors, four DELLA proteins were recovered (RGL1 twice, RGL2, and RGA). RGL2 and RGA were in frame with the GAL4 activation domain (AD) but were lacking the DELLA protein domain. The two RGL1 clones were not in frame with the GAL4-AD but contained the DELLA domain; inclusion of the DELLA domain may have promoted transcriptional activation without the need of the GAL4-AD (de Lucas et al., 2008). We then proceeded to reverify the interactions in yeast by cloning the full-length ORFs of all five *DELLAs* in frame with the GAL4-AD in the yeast vector pGADT7. All five DELLA proteins showed strong interactions with ENY on both low (plasmid selection only) and high (selecting for the protein:protein interaction) stringency plates containing the chromogenic marker X-α-Gal (Figure 8A). Quantification of the ENY-DELLA interaction using a β-galactosidase activity assay verified strong interactions compared with the negative controls (see Supplemental Figure 17A online).

To independently verify the interaction of ENY with each DELLA protein, we performed bimolecular fluorescence complementation (BiFC) assays in *Nicotiana benthamiana* leaf epidermal cells. Before attempting BiFC assays, the subcellular localization of yellow fluorescent protein (YFP)-ENY was confirmed by transient expression in *N. benthamiana* leaf epidermal cells. Consistent with previous reports on the IDD family (Welch et al., 2007; Wong and Colasanti, 2007), eYFP-ENY was nuclear localized (see Supplemental Figure 18 online). Since the GAL4 fusions in the yeast two-hybrid experiment were on the N terminus of the protein, the amino acids 1 to 174 of YFP were fused to the N terminus of ENY. Similarly, the amino acids 175 to 239 of YFP were fused to the N terminus of each of the DELLA proteins. The highest fluorescence in the negative controls occurred when the two halves of YFP were both fused to ENY; however, this signal was very weak compared with the $YFP_{1\text{-}174}$-ENY and $YFP_{175\text{-}end}$DELLA signals. All ENY-DELLA interaction combinations showed high and consistent fluorescent signals except GAI; however, GAI was still slightly higher than background fluorescence (Figure 8B; see Supplemental Figure 17B online). The interaction of ENY with DELLA proteins, via both the yeast two-hybrid and BiFC approaches, demonstrated a mechanistic and functional context for ENY: that DELLA proteins may modulate ENY function and/or that ENY may modulate DELLA function.

ENY Modulates the Expression of *DELLAs* and *SCL3* during Seed Development

To further investigate the connection of ENY and DELLA function, we measured *DELLA* expression during seed development in Columbia wild type and *ENY* transgenic lines (Figure 9). First, *RGL1* and *RGL3* expression levels were similar between Columbia wild type and all *ENY* transgenic lines. In addition, *DELLA* expression in Columbia wild type and the *RAB18*:*ENYami* knockdown line was generally similar. However, there were clear differences in *RGA*, *GAI*, and *RGL2* in *ENY-ME* and *RAB18*:*ENY* transgenic lines. In the *ENY-ME* line, *RGA* levels increased sharply between 9 and 18 DPA and were still slightly elevated in mature harvested seed. In the *RAB18*:*ENY* line, increased *RGA* levels were seen only from 15 DPA onwards, somewhat paralleling the later increase in *ENY* seen in the *RAB18* lines (Figures 1 and 9). Both *GAI* and *RGL2* expression increased during 12 to 18 DPA in both *ENY-ME* and *RAB18*:*ENY*, and *RGL2* was still elevated >2-fold in mature harvested seed in both *ENY-ME* and *RAB18*:*ENY* lines.

Previous studies identified *SCL3* as a GA-repressed and DELLA-induced transcript (Zentella et al., 2007). More recently, *SCL3* function has been further defined to include a positive regulatory role in GA signaling, including an SCL3 and DELLA antagonism and role in root cell elongation and ground tissue maturation (in a regulatory pathway defined with SHORTROOT [SHR], SCARECROW [SCR], and DELLAs) (Heo et al., 2011; Zhang et al., 2011). Since *SCL3* was downregulated in the *RAB18*:*ENY* induction experiment (Figure 4; see Supplemental Data Set 2 online), we profiled its expression during seed development. In Columbia wild type, *SCL3* expression increased during seed development and was highest in the mature harvested seed (Figure 9). In *ENY-ME*, *SCL3* abundance was lower than Columbia wild type between 6 and 12 DPA but rose to wild-type levels from 15 DPA to mature harvested seed (paralleling the increase in DELLAs GAI and RGL2). *RAB18*:*ENY*, on the other

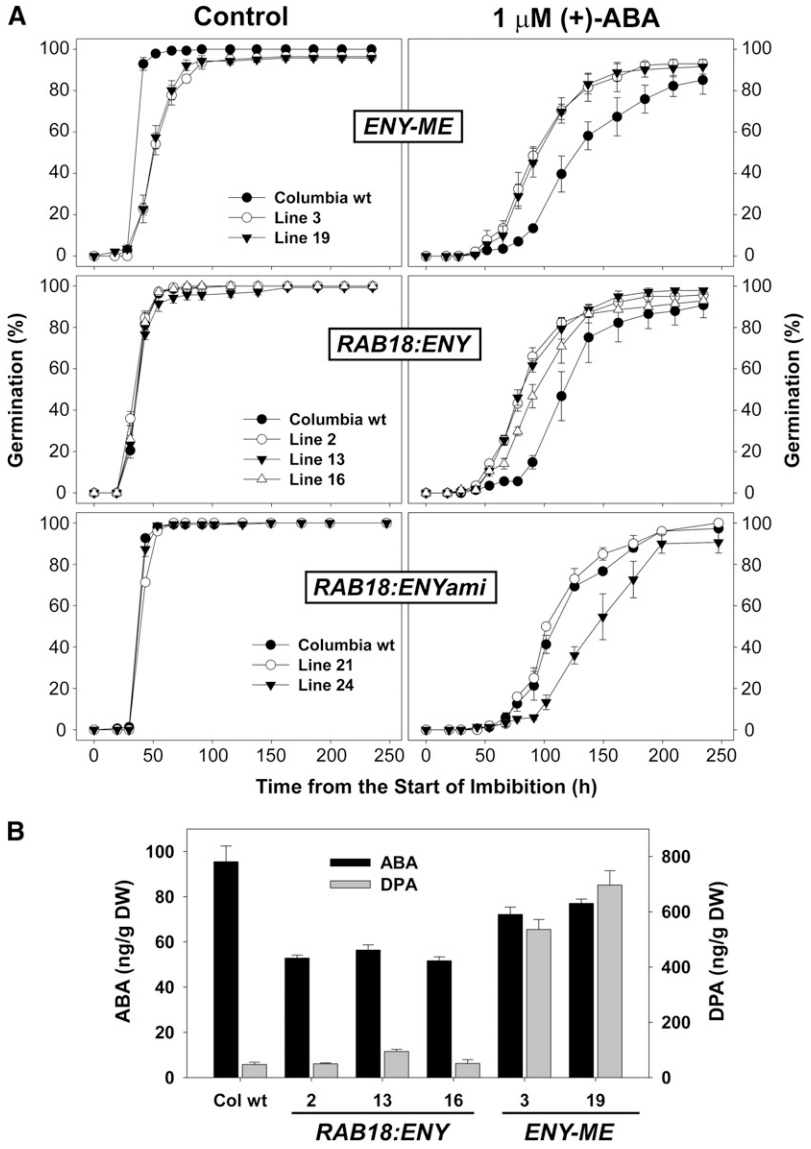

Figure 7. ENY Antagonizes ABA Synthesis and Signaling.

(A) Germination sensitivity to applied (+)-ABA at 1 μM concentration in Columbia wild type (wt), overexpression *ENY-ME* and *RAB18:ENY* lines, and knockdown *RAB18:ENYami* lines. Seeds were plated and placed directly in germination conditions. Error bars equal the SE of 3 × 50 seeds.
(B) Amounts of ABA and its metabolite dihydrophaseic acid (DPA) in Columbia wild type and overexpression *ENY-ME* and *RAB18:ENY* lines. Error bars equal the SE of 3 × 50 mg dry weight (DW) mature seed.

hand, was similar to the wild type at 6 and 9 DPA, when the *RAB18* promoter was not as active, and then dropped to considerably lower levels than Columbia wild type through the rest of seed development and also in the mature harvested seed. The *RAB18:ENYami* line displayed the opposite trend at 15 and 18 DPA; *SCL3* levels were higher than Columbia wild type (Figure 9).

DISCUSSION

Only four members of the *Arabidopsis* IDD family have been linked to a physiological role. Three members, *NUTCRACKER/IDD8* (*NUT*), *MAGPIE/IDD3* (*MAG*), and *JACKDAW/IDD10* (*JKD*), are involved in a regulatory loop with the GRAS domain proteins *SHR* and *SCR* associated with *Arabidopsis* root development and patterning. *SHR* has been shown to directly regulate *NUT* and *MAG* expression, while MAG and JKD have been shown to physically interact with SHR and SCR (Levesque et al., 2006; Cui et al., 2007; Welch et al., 2007). Recently, Seo et al. (2011) found that *NUT/IDD8* regulates the transition to flowering through its regulation of sugar metabolism. *SHOOT* GRAVITROPISM5/*IDD15* (*SGR5*) has been linked to gravity perception and starch accumulation in inflorescence stems (Tanimoto

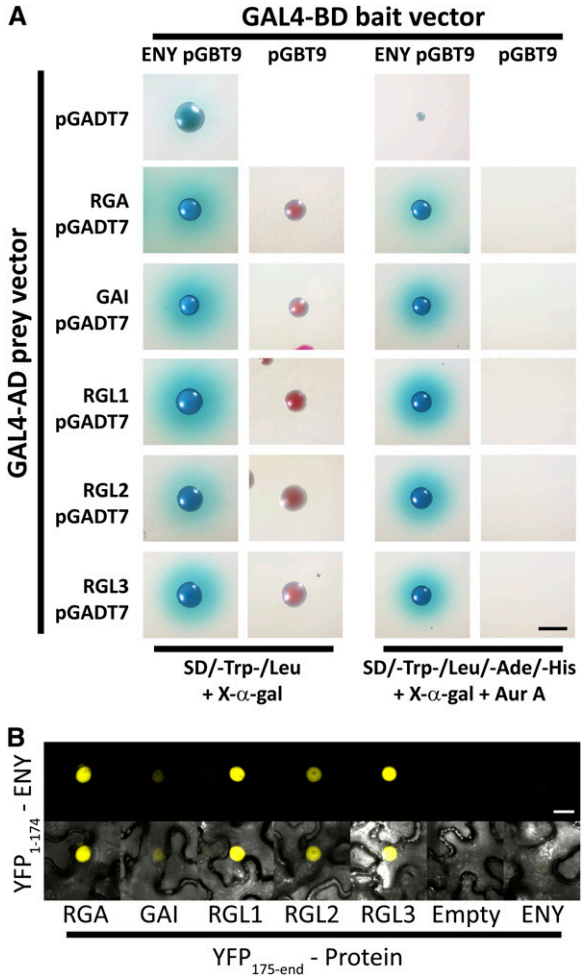

Figure 8. ENY Physically Interacts with DELLA Proteins.

(A) Yeast two-hybrid analysis of the interaction between ENY and DELLAs, RGA, GAI, RGL1, RGL2, and RGL3, on low (plasmid selection only) and high stringency plates (protein–protein interaction selection markers included Ade and His and the antibiotic Aureobasidin A [Aur A]). In addition, blue color is indicative of protein–protein interaction and is the result of α-galactosidsase activity. Bar = 400 μm.

(B) BiFC of the interaction between ENY and DELLAs, RGA, GAI, RGL1, RGL2, and RGL3, in *N. benthamiana* leaf epidermal cells. Top panel presents the signal from eYFP, reconstituted from $YFP_{1\text{-}174\ aa}$-ENY and each $YFP\text{-}_{175\text{-}end\ aa}$-DELLA. Bottom panel includes eYFP and transmitted light detector signals. Bar = 20 μm.

et al., 2008). Interestingly, the *endodermal-amyloplast less1* mutant, which has a one amino acid deletion in *SHR*, was found to regulate *SGR5* expression in inflorescence stems (Morita et al., 2007). While *ENY* has not been linked to *SHR* or *SCR* action, we connected ENY action to DELLA proteins that are also members of the GRAS (for GAI, RGA, and SCR) family of transcriptional regulators (Sun, 2008). Thus, one common theme in the *Arabidopsis* IDD family is the capacity to interact, either physically or genetically, with members of the GRAS family.

ENY Causes Feedback Downregulation of GA Homeostasis

We were confronted with an apparent inconsistency in *ENY* function that there was (1) a positive relationship to GA signaling through FR/R light germination and hypocotyl growth experiments versus (2) the opposite negative regulatory role of *ENY* on the expression of GA metabolism and signaling genes. Two possibilities were considered: (1) ENY promotes GA-associated downstream signaling events (e.g., expression of *EXPA1*) but at the same time inhibits upstream GA synthesis and signaling (e.g., expression of *GA3ox1*), or (2) ENY promotes GA-associated downstream signaling events and, because of this (as a secondary effect), feedback regulation is engaged to counteract perceived increases in GA signaling. After reviewing the literature on GA synthesis and signaling, it became evident that the second hypothesis was more likely.

Feedback regulation of GA homeostasis has been well documented. For example, *GA3ox* and *GA20ox* expression was elevated in GA biosynthetic mutants and decreased by GA treatment in the mutants or wild type (Cowling et al., 1998; Xu et al., 1999). By contrast, *GA2ox* expression was decreased in the *ga1-2* biosynthetic mutant and increased upon GA treatment (Thomas et al., 1999). More recently, when RGA was induced via a glucocorticoid-dexamethasone–inducible system in seedlings, the GA biosynthesis genes *GA3ox1* and *GA20ox2* and GA receptors *GID1A* and *GID1B* were upregulated. One hour of GA treatment in 8-d-old *ga1-3* seedlings resulted in downregulation of these two biosynthetic genes and two GA receptor genes (Zentella et al., 2007). Thus, applied GA or mutations that increase GA signaling (e.g., *gai-t6* and *rga-24*) result in negative feedback regulation. Inhibition of GA synthesis or mutations that decrease GA signaling (e.g., *gai*) result in positive feedback regulation of GA homeostasis (Sun, 2008). Consistent with the theme of *ENY* feedback regulation, five (*GA4*, *GA20ox2*, *SCL3*, *AT4G19700*, and *GID1B*) of the top six genes that Zentella et al. (2007) identified as GA downregulated and DELLA upregulated were also downregulated by *ENY* during induction experiments (see Supplemental Data Set 2 online). Additional observations suggesting feedback regulation were the changes in the upstream GA biosynthesis genes, *GA2* and *GA3*, and in other downstream genes, such as *GA3ox2* (*GA4H*), that have not previously been reported to be involved in feedback regulation (Yamaguchi et al., 1998; Helliwell et al., 1998; Matsushita et al., 2007). *GA2* and *GA3* were downregulated in imbibed seeds of *RAB18:ENY* line 13, and *GA3ox2* was downregulated when *ENY* was induced with ABA with even greater repression under ABA/GA treatment compared with Columbia wild type (Figure 3B; see Supplemental Table 1 online).

Matsushita et al. (2007) isolated a protein, AT-HOOK PROTEIN OF GA FEEDBACK1 (AGF1), which bound to a *cis*-acting DNA motif, GNFEI, named for its role in the GA feedback mechanism. Overexpression of *AGF1* promoted the positive feedback loop (upon inhibition of GA synthesis) and counteracted the negative loop (upon GA treatment). Interestingly, expression of *AGF1* is downregulated 2-fold in 3-h imbibed seeds of *RAB18:ENY* line 13 (see Supplemental Data Set 3 online). This suggests that the presence of *ENY* acted to curtail the modulation of feedback

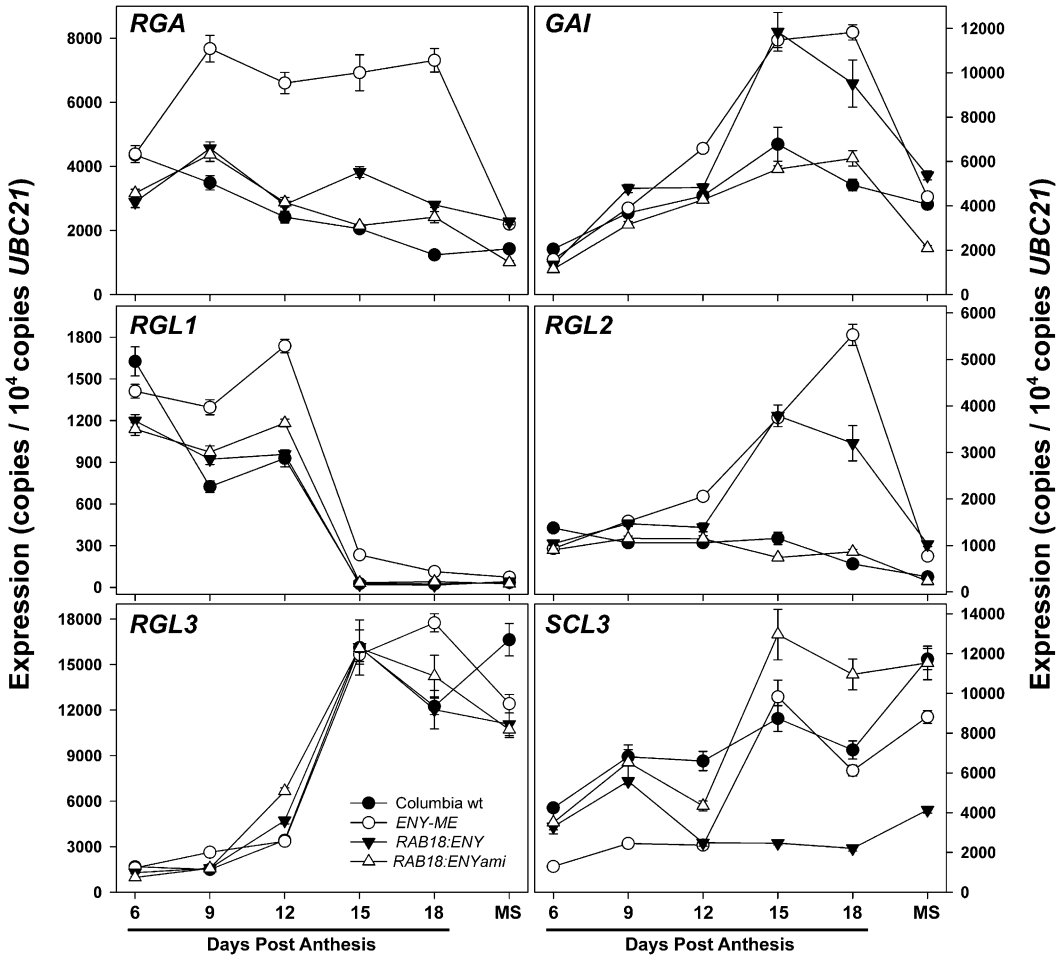

Figure 9. *DELLA* and *SCL3* Expression Is Altered by *ENY* Overexpression during Seed Development.

Expression of *RGL2*, *RGA*, and *GAI* was markedly altered when *ENY* expression was increased using the 2x35S or *RAB18* promoters (*ENY-ME* and *RAB18*:*ENY*, respectively). By contrast, *DELLA* expression during *ENY* knockdown (*RAB18*:*ENYami*) was similar to that of the Columbia wild type (wt). *SCL3* expression displayed opposite trends compared with the *DELLAs*. *SCL3* was downregulated in *ENY-ME* and *RAB18*:*ENY* lines. However, in *ENY-ME*, *SCL3* expression returned to wild-type levels during the time when *RGL2* and *GAI* increased. Error bars represent the SE of two biological replicates. Data were normalized to 10^4 copies of *UBC21*. Transgenic lines used for analysis included *ENY-ME* line 3, *RAB18*:*ENY* line 13, and *RAB18*:*ENYami* line 24. MS represents mature harvested seed.

through AGF1 (i.e., the plant wanted greater negative feedback inhibition of GA homeostasis, so *AGF1* was downregulated).

To our knowledge, increased *ENY* transcription resulted in one of the most comprehensive changes in the GA signaling pathway reported in the literature; the only major signaling factor that was not changed in any of our experiments, if we consider redundancies in gene families, was *SPY*. In tobacco, the basic Leu zipper REPRESSION OF SHOOT GROWTH (RSG) has been found to repress accumulation of GA through regulation of ent-kaurene oxidase and negative feedback regulation of *GA20ox1* (Fukazawa et al., 2010). In rice (*Oryza sativa*), *YABBY1* is also involved in negative feedback regulation of *GA3ox2* (Dai et al., 2007). Feedback regulation may be related to ENY's interaction with DELLA proteins; the consequences of this antagonistic interaction are discussed below.

Ectopic *ENY* Overexpression Delays Seed Maturation Events

Several lines of evidence suggest *ENY* modulates and counteracts the maturation process regulated by ABA (Santos-Mendoza et al., 2008). First, 35S misexpression lines exhibit delayed maturation processes, particularly senescence in the seed coat and endosperm. This phenotype seems related to upregulation of *ENY* during early seed development. It was not observed in *ENY* lines driven by the *RAB18* promoter, which increased *ENY* expression above wild-type levels much later in seed development when events such as endosperm assimilation were almost complete (Figure 1; see Supplemental Figure 8 online). Although the *ENY-ME* phenotype is unique, it has similarities to *fus3*, *abi3*, *lec2*, and *lec1* mutants (Nambara et al., 1992; Keith et al., 1994;

West et al., 1994; Stone et al., 2001), in all of which there is a delay or absence of maturation events (Holdsworth et al., 2008). In *ENY-ME* lines, seed desiccation was delayed and occurred abruptly; this is reminiscent of the desiccation intolerance of *fus3*, *abi3*, and *lec1* mutants. However, as in weak *abi3* and *lec2* mutants (Ooms et al., 1993; Stone et al., 2001), the majority of *ENY-ME* seed were tolerant to desiccation at maturity. The second resemblance to *fus3*, *abi3*, *lec2*, and *lec1* mutants was the accumulation of lower and altered levels of storage compounds. *ENY-ME* lines had reduced levels of protein reserves and increased accumulation of starch and endosperm-specific fatty acids. *FUS3* mutants, for example, also display increased levels of starch and lower protein content (Tiedemann et al., 2008). As starch is usually transitory in wild-type *Arabidopsis* (Focks and Benning, 1998), the presence of starch in mature *ENY-ME* seeds suggests that normal reserve partitioning was not completed before desiccation. Similarly, seed coat and endosperm development was delayed and, at least with respect to the seed coat, was not completed before seed desiccation. This is evidenced by the failure of mucilage to extrude from the seed coat upon imbibition and the presence of increased endosperm-specific fatty acids.

From changes in gene expression in *ENY* overexpressing seed (see Supplemental Data Set 1 and Supplemental Table 1 online), it can be seen that *ENY* downregulated the maturation-promoting factor *FUS3*, which was correspondingly upregulated in the *ENY* knockdown line. However, the effects of *ENY* expression on *FUS3* were moderate and confined to late maturation and early imbibition as no changes were detected at 10 DPA, a time when *FUS3* is highly expressed. Nonetheless, *ENY*'s regulation of *FUS3* is consistent with *ENY* being a modulator of maturation and subsequent germination, as *FUS3* has been found to repress GA synthesis and induce ABA production (Gazzarrini et al., 2004; Curaba et al., 2004). Conversely, *ABI1*, a negative regulator of the ABA response, was positively influenced by *ENY* (see Supplemental Data Set 1 and Supplemental Table 1 online). *ABI1* is a member of a group of protein phosphatase type-2C proteins that are negative regulators of ABA-related responses (Yoshida et al., 2006). ABI1 family members, SUCROSE NONFERMENTING 1-RELATED PROTEIN KINASE2 (SnRK) proteins, and the recently discovered ABA receptor family of PYRABACTIN RESISTANCE (PYR)/PYR-LIKE (PYL)/REGULATORY COMPONENT OF ABA RECEPTOR proteins have been shown to interact directly in an ABA regulatory hub (Fujii et al., 2009; Park et al., 2009). *PYL11* was in our DEG list in *RAB18 ENY* overexpression and knockdown lines and changed in parallel with *ABI1*. The precise role PYL11 may play in ABA signaling has not been revealed (Park et al., 2009).

ABA accumulation was also reduced in mature seeds of *ENY* overexpression lines, and ABA sensitivity was negatively associated with *ENY* transcription (i.e., *ENY* overexpression lines were ABA hyposensitive, and knockdown lines were hypersensitive compared with Columbia wild type) (Figure 7; see Supplemental Figure 16 online). These data suggest ENY acts antagonistically to ABA; in view of the direct relationship between ABA and seed maturation, it is consistent that ENY negatively affects maturation.

ENY Promotes Germination and Selectively Regulates Growth-Associated Factors

Evidence for positive regulation of germination by *ENY* is that *ENY-ME* and *RAB18-ENY* seed germination is insensitive to FR light (see Supplemental Figure 14 online), that *RAB18*:*ENYami* seed germination is FR hypersensitive and R insensitive (see Supplemental Figure 14 online), and gene expression profiles are consistent with ENY mediating red light and GA signaling (Figure 6). Given the skotomorphogenic-like phenotype under GA treatment, the ENY-DELLA interaction, and feedback-like effects on GA homeostasis, ENY seems to be related to GA and growth-associated signaling. Moreover, *ENY* also repressed expression of the GATA-type transcription factor *GNC* (expression was decreased in *ENY-ME* and *RAB18*:*ENY* and increased in the *RAB18*:*ENYami* knockdown) (see Supplemental Table 1 online). *GNC* expression is repressed by GA application and elevated in *ga-1* and *gid1abc* mutants. GNC and its homolog GNC-LIKE function as repressors of GA action, inhibiting germination and elongation growth and promoting greening (Richter et al., 2010). A close association of ENY with the GA pathway is also consistent with the fact that phytochrome functions to activate GA synthesis during germination but attenuates GA action during photomorphogenesis (Yamaguchi et al., 1998; Achard et al., 2007; Feng et al., 2008; Strasser et al., 2010).

In addition to GA, *ENY* also regulated the brassinosteroid pathway, which is known to be involved in the promotion of growth and cell elongation (see Supplemental Table 1 online). *BAS1* and *SOB7*, whose activation-tagged mutants were recovered in suppressor screens for *phyB*, metabolize the brassinosteroids (BRs) brassinolide and castasterone to inactive products through hydroxylation (Turk et al., 2005). As suppressors for *phyB*, *BAS1* and *SOB7* negatively regulate hypocotyl elongation and cotyledon area (Turk et al., 2005). In *RAB18*:*ENY* imbibed seeds, both *BAS1* and *SOB7* were downregulated, consistent with *ENY* being a promoter of growth, in this case via BRs. BRs are also inactivated by glucosylation through the *DOGT1* gene product (Poppenberger et al., 2005), which was downregulated in *RAB18*:*ENY* seeds. However, the biosynthetic gene *BRASSINOSTEROID-6-OXIDASE2* (*BR6ox2*), which catalyzes the last committed steps to active brassinolide, was also downregulated in *RAB18*:*ENY* imbibed seeds; however, this could be the result of feedback inhibition. *BR6ox2* was also downregulated during GA treatment of *ga1-3* seedlings (Zentella et al., 2007).

ENY Interacts with DELLA Proteins and Causes Feedback-Like Regulation of *DELLA* Transcripts during Seed Development

Integration of light and GA signaling was demonstrated by de Lucas et al. (2008) and Feng et al. (2008), who showed that DELLA and PIF directly interact to create a regulatory node that modulates plant growth. Both groups demonstrated how postgerminative seedling growth in light and dark conditions is modulated by the DELLA-PIF interaction and revealed how DELLAs may exert their effects on transcription to restrain growth. The two groups demonstrated that the DELLA-PIF interaction blocked the transcriptional activation function of PIFs; thus, in the light, when GA

levels are low and DELLA concentrations are high, DELLAs would abrogate PIF-promoted processes, such as cell elongation. The effects of PIFs are also blocked by interaction with activated Pfr phytochromes, such as PHYB, which subsequently tag the PIF for proteasomal degradation (Al-Sady et al., 2006; Shen et al., 2007). In the dark, without the activated PHYs to curtail their action, PIFs and associated factors promote GA accumulation; high GA levels promote the proteasome-mediated degradation of DELLAs via the action of the $^{GID1\text{-}SLY1}$SCF E3 ubiquitin ligase complex; thus, PIFs are released (Griffiths et al., 2006). The identification of additional DELLA interactors has also furthered our knowledge of how DELLAs act as global repressors of development and growth. During silique development, ALC is involved in defining the separation layer responsible for fruit opening. It has been suggested that DELLA interaction with ALC blocks its action and, thus, separation layer formation (Arnaud et al., 2010). Hou et al. (2010) demonstrated that DELLAs interact physically with JAZ1 to compete with and block the JAZ1-MYC2 interaction, thus allowing MYC2 to perform its functional role as an activator of JA responses. More recently, it was shown that SCL3 is a positive regulator of the GA response and that its interaction with DELLAs modulates GA homeostasis, creating an antagonistic relationship (Zhang et al., 2011).

So how does ENY functionality fit within the context of DELLA function? Given the opposing regulatory effects of ENY and DELLAs, their direct interaction suggests a similar antagonistic relationship to that of SCL3. Thus, ENY may block DELLA action by disrupting DELLA protein interactions, thereby allowing factors, such as PIFs, to function. Alternatively (or in addition), DELLAs may inhibit ENY action. Future experiments will identify which genes ENY directly regulates and the importance of DELLA interaction to ENY function.

The increase of *RGA*, *GAI*, and *RGL2* expression during seed development, particularly during late maturation, in *ENY-ME* and *RAB18:ENY* lines also suggests an ENY-DELLA antagonism. Given the results from the *RAB18:ENY* induction experiments that showed negative-feedback regulation of GA homeostasis, the increase in *RGA*, *GAI*, and *RGL2* during seed maturation could suggest that the increase in *ENY* expression is being balanced by DELLA-mediated feedback effects. *RGL2*, *RGA*, and *GAI* are the main DELLAs that have been identified as repressors of germination (Lee et al., 2002; Tyler et al., 2004; Piskurewicz et al., 2009). More specifically, *RGL2*, *RGA*, and *GAI* are involved in the repression of testa and endosperm rupture and promote the maintenance of endogenous ABA and ABI5 levels in the imbibed seed (Piskurewicz et al., 2008, 2009). Recently, it was shown that an RGL2-dependent release of ABA in the endosperm helps regulate embryo growth in dormant seeds (Lee et al., 2010).

A role for DELLAs in balancing ENY function and the strict negative-feedback inhibition on GA homeostasis that we observed may explain why alterations to *ENY* transcription in overexpression lines did not produce stronger phenotypes. With respect to *ENY* knockdown lines, the subtle phenotypes observed can likely be attributed to the lack of complete knockout in *ENY* transcription and the genetic redundancy created by other members of the *IDD* family.

Integrating the evidence we have compiled, we present a model of ENY function during seed maturation and early germination (Figure 10). In the simplest terms, *ENY* functions to promote GA-associated responses and repress ABA responses (or rather, subsets of those responses). However, our observations suggest a more complex effect, which includes changes in other hormonal pathways. In addition, *ENY* may promote select

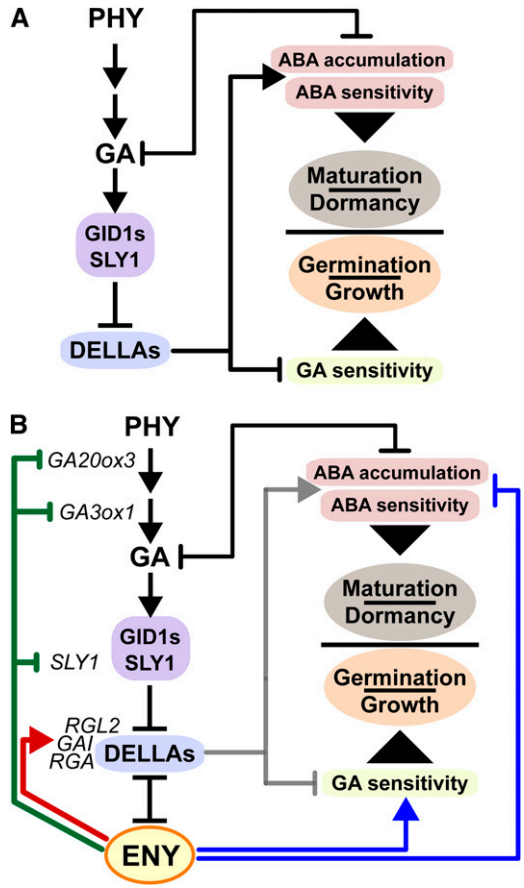

Figure 10. Proposed Model of ENY-DELLA Interaction during Seed Maturation and Early Germination.

(A) During seed maturation, ABA works antagonistically to GA and helps prevent GA accumulation. Upon light, imbibed mature seeds accumulate GA in a phytochrome (PHY)-dependent manner. GA triggers proteosome-mediated degradation of DELLAs, such as RGL2 via the GA receptor/SLY1 interaction. If DELLAs (RGL2, RGA, and GAI) are permitted to accumulate, they, in turn, promote maintenance of ABA levels that contribute to blocking germination (Zentella et al., 2007; Piskurewicz et al., 2008, 2009). For simplicity, other key factors, such as PIL5, ABI5, ABI3, or SCL3, were left out of the model.

(B) ENY has the capacity to increase GA sensitivity while decreasing ABA sensitivity and accumulation; ENY may partially accomplish this through modulation of DELLA activity. However, the presence of *ENY* also causes immediate feedback effects, which result in downregulation of GA synthesis and signaling and upregulation of *DELLAs* themselves. The blue lines indicate that ENY may also directly regulate the GA and ABA response. Whether or not a consequence of DELLA-ENY interaction, the downregulation of GA homeostasis mediated by ENY would be advantageous during maturation; ENY would help ensure that GA synthesis is repressed. However, the interaction of ENY with DELLAs would allow it to modulate GA sensitivity for subsequent germination.

maturation-associated processes, such as the repression of photosynthetic events. Finally, although we propose that *ENY* is a positive regulator of growth, it also strongly downregulates GA synthesis and signaling. Thus, *ENY* creates a situation that reinforces repression of GA synthesis (an important action during seed maturation) but at the same time, and perhaps partially as a consequence of DELLA antagonism, promotes events important to subsequent germination.

METHODS

Plant Materials, Growth Conditions, and Generation of Transgenic Plants

Growth of *Arabidopsis thaliana* ecotype Columbia occurred in a growth chamber with a 16-h-light/8-h-dark cycle at 22°C under 150 to 175 μmol/m^2/s light intensity for production of transgenic plants and seed collection. Transformation of *Arabidopsis* using the *Agrobacterium tumefaciens* strain GV3101:pMP90 followed Clough and Bent (1998). Single-gene-copy homozygous transgenic seed was carried through to the T2, T3, or T4 generation for subsequent phenotypic analyses. When comparing Columbia wild-type seed to *ENY* transgenic lines, seed was always grown at the same time and in the same growth chamber to ensure the most direct comparison was made. For overexpression of *ENY*, the *ENY* ORF was PCR amplified from seed cDNA and recombined into pDONR221 (Life Technologies). Next, the *ENY* ORF was recombined into the 2x35S expression vector pMDC32 (Curtis and Grossniklaus, 2003). The *RAB18* promoter was also used to drive expression of *ENY* or an amiRNA designed for *ENY*. A 659-bp fragment of the *RAB18* promoter was amplified from Columbia genomic DNA with *Sbf*I and *Kpn*I restriction sites and cloned into pCR2.1-TOPO (Life Technologies) before restriction digestion and ligation into pMDC32 to replace the 2x35S promoter. For GUS expression, a 2946-bp fragment of the upstream region of *ENY* was cloned in pDONR221 before being recombined into pMDC162 (Curtis and Grossniklaus, 2003). An amiRNA based on the mir319a backbone was designed using Web MicroRNA Designer 2 (Schwab et al., 2006) and cloned into pDONR221 before cloning into the expression vectors pMDC32 and pMDC32-*RAB18*. Please refer to Supplemental Table 2 online for a list of PCR primers.

Seed Fresh/Dry Weight Analysis during Development

Flowers from ~90 to 100 plants of Columbia wild type and *ENY* misexpression lines were labeled at the time of anthesis with colored tape. Approximately 20 seeds were dissected from two to three siliques and collected in prebaked and preweighed screw-cap HPLC glass vials (Agilent). For weighing, a scale capable of stably measuring 10^{-5} g was used. Following fresh weight measurement, seeds were baked for 24 h at 110°C and allowed to cool to room temperature in a desiccator before dry weight was measured.

Seed Mucilage Staining

To stain the acidic polysaccharides in *Arabidopsis* mucilage, mature seed of *ENY* misexpression lines were stained in 0.03% ruthenium red (Sigma-Aldrich) for ~2 to 3 min. Seeds were then rinsed with water and mounted on microscope slides before pictures were captured using a Zeiss SteREO Lumar.v12 stereomicroscope equipped with a 3.3 MP Zeiss ICc3 digital camera. In addition to ruthenium red, the fluorescent polysaccharide binding calcofluor white (American Cyanamid) was used to stain mature seeds. A stock solution of 20 mg/mL calcofluor white in 40 mM NaOH was diluted 20-fold in water to make a working solution of 1 mg/mL, and seeds were stained for ~5 min before rinsing with water twice. Seed images were captured with the above mentioned microscope and a 4',6-diamidino-2-phenylindole filter set. For EDTA treatment of *2x35S:ENY* seeds, the procedure followed that described by Arsovski et al. (2009).

Resin Embedding for Light Microscopy

Resin embedding of Columbia wild type and *ENY-ME* lines followed Western et al. (2000) with modifications. Developing seeds at 6 to 10 DPA, enclosed within partially opened siliques, were fixed with 3% paraformaldehyde (Sigma-Aldrich) and 1.25% glutaraldehyde (Sigma-Aldrich) in 0.5 M sodium phosphate buffer, pH 7.0, overnight at 4°C. Following brief rinses with phosphate buffer, the seeds were dehydrated in a graded ethanol series for 5 d. The seeds were then gradually infiltrated with LR White resin (Ted Pella) over a period of 5 d. LR White was polymerized at 57°C in gelatin capsules for 24 h. Seeds were sectioned at 1 μm on a Leica RM2165 microtome before mounting on Probe-On Plus slides (Fisher Scientific). Sections were stained briefly with 1% (w/v) toluidine blue O in 1% (w/v) sodium borate, pH 11.0, before sealing with VectaMount mounting medium (Vector Labs). Pictures were captured using a ×20 objective on a Leica DMR microscope and MacroFire CCD camera (Optronics).

GUS Staining during Seed Development

Siliques were labeled and seed was collected at 3, 6, 9, 12, 15, and 18 DPA and fixed in 20% acetone for >24 h at −20°C. The same procedure was followed for seeds collected after various stages of imbibition and germination. Seeds were opened to allow easier access to the GUS reagent. Following a brief vacuum infiltration, seeds were incubated in 0.1 M $NaPO_4$, pH 7, 10 mM EDTA, 0.1% Triton X-100, 1.5 mM $K_3Fe(CN)_6$, 0.5 mM $K_4Fe(CN)_6$, and 2.0 mM X-Gluc (Rose Scientific) for 30 min to 1 h at 37°C. Seeds were preserved in 70% ethanol before capturing images with the Leica and Zeiss microscopes detailed above.

Vertical Agar Plate Growth Assays

Following surface sterilization in 70% ethanol and 10% commercial bleach, and two rinses with sterile water, seeds were resuspended in 0.2% agar. Columbia wild type and *2x35S:ENY* T3 seeds were placed on 0.5 MS, 2 mM MES, pH 5.8, plus 1% agar with or without the addition of 1% Suc at a density of 12 to 15 seeds per plate (10 × 1.5-cm square plates; BD Falcon). Seeds were moist chilled for 5 d before plates were placed at 22°C for 7 d (16-h-light/8-h-dark cycle; 70 to 80 μmol/m^2/s). A Canon Powershot G10 camera was used to capture images before measurement in ImageJ (Abràmoff et al., 2004).

For *ENY* induction experiments with ABA, T2 transgenic lines of *RAB18:ENY* were plated at a density of ~20 seedlings per plate on 0.5 MS, 2 mM MES, pH 5.8 plus 1% agar. Following 3 d of moist chilling and 5 d under germination conditions (as above), seedlings were transferred to plates containing 10 μM (+)-ABA and left on the plates for 1 to 6 h. In a separate experiment, used for qRT-PCR expression analysis, seedlings were collected following a 3-h treatment on plates containing ABA with or without the inclusion of 10 μM GA_3 or 1 μM Paclobutrazol (Sigma-Aldrich).

RNA Extraction

The following tissue amounts from *Arabidopsis* were generally used for RNA extraction: 50 to 100 siliques containing seeds for time points during seed development, 40 to 50 mg fresh weight of dry mature seed (including those time points that were extracted following imbibition), or 24 to 32 5-d-old seedlings. All tissues were frozen in liquid N_2 prior to grinding. For dry and imbibed seeds, frozen tissue was equilibrated with RNA*later*-ICE

(Life Technologies) for 3 to 5 d prior to spinning down, resuspending in RNA extraction buffer, and grinding with a ceramic sphere (Q-Biogene) in a FASTPrep FP120 tissue homogenizer (Q-Biogene). RNA extraction from seedling tissue used the RNeasy Mini Kit following the manufacturer's protocol (Qiagen). The RNA extraction procedure for any seed tissues followed Fei et al. (2007) with minor modifications, including adjustment of the volumes for use with the RNeasy Mini Kit or RNeasy Midi Kit (Qiagen) and an additional 7.5 M LiCL precipitation (Life Technologies).

RNA, used for qPCR expression analysis of genes during seed development, was extracted from seeds removed from four to six siliques. For 6 to 18 DPA time points, seeds were incubated in RNA*later* solution (Life Technologies) at 4°C for 4 to 5 d prior to storage at −20°C before extraction. RNA was extracted using an RNAqueous kit with Plant RNA Isolation Aid according to the manufacturer's protocol (Life Technologies). Following RNA extraction, RNA was treated with DNase using the TURBO DNA-free kit (Life Technologies). RNA quality was analyzed with an RNA Nano chip using the Bioanalyzer 2100 (Agilent) prior to cDNA synthesis.

Gene Expression Analysis

For cDNA synthesis, 1 μg of RNA was used with the Superscript III First-Strand Synthesis Supermix for qRT-PCR (Life Technologies) according to the manufacturer's instructions except that the cDNA synthesis reaction was increased to 60 min. cDNA was diluted 12.5-fold in water, and 2 to 8 μL of this dilution was used for qRT-PCR expression analysis. For qPCR, SYBR GreenER qPCR Supermix Universal (Life Technologies) was used in a total reaction volume of 25 μL, with 0.1 μL ROX reference dye and 0.2 μM primer concentration. Data were collected as Ct values in an MX3000P instrument with MXPro v4.1 software using the SYBR Green program with dissociation curve (Agilent). Relative fold change was calculated using the cycle threshold (CT) $2^{-\Delta\Delta CT}$ method (Pfaffl, 2001). Primers used for qRT-PCR are listed in Supplemental Table 2 online. *ACT2* or *UBQ11* were used to normalize gene expression for seedling tissue and imbibed seeds, respectively. Expression data in Figure 3 were expressed as log2 before inputting into Heatmap Builder (King et al., 2005).

For qPCR gene expression measurements during seed development, 900 ng of RNA was used with the SuperScript VILO cDNA synthesis kit with a synthesis reaction of 65 min. cDNA was diluted 14-fold in water, and 5 μL of this dilution was used in each qPCR reaction. qPCR was performed as detailed above. To obtain copy numbers for gene expression, the formula mass (g) = DNA (bp) * 1 mole/6.023 × 10^{23} molecules (bp) * 660 g/mole was used to equate the plasmid mass with DNA base pair size (660 was used as the average weight for a double-stranded DNA molecule). Linearized plasmid templates, including the *ENY*, *RGA*, *GAI*, *RGL1*, *RGL3*, and *SCL3* ORF or *RGL2* cDNA, were used as templates and standard curves varying from 300,000 to 30 copies were generated. Standard curves relating copy number to CT values were generated alongside the experimental samples. *UBC21* was selected as a reference gene based on Czechowski et al. (2005).

Microarray Analysis of *ENY* Transgenic Lines

RNA samples for microarray analysis were extracted from two biological replicates that were set up and collected independently. Thus, each microarray time point consisted of two biological replicates and two to three technical replicates, which included dye-swaps (thus, four slides per time point was the minimum). Two color array experiments were performed using arrays based on the Operon *Arabidopsis* Genome Array Ready Oligo Set (AROS) Version 3.0 (http://omad.operon.com/download/index.php) and were obtained from D.W. Galbraith's Lab at the University of Arizona (http://ag.arizona.edu/microarray/). Two color microarray experiments were always a transgenic *ENY* line compared with Columbia wild type.

Generally, 1 μg of RNA was used with the Amino Allyl MessageAmp II aRNA amplification kit (Applied Biosystems) to produce amplified antisense RNA (aRNA). Five micrograms of Alexa 555 and 647 (Life Technologies) labeled aRNA was hybridized to *Arabidopsis* 70mer oligonucleotide microarray slides. A microarray slide covered with a LifterSlip (Erie Scientific) was placed into a hybridization chamber (Arrayit). The hybrization solution consisted of 70 μL of SlideHyb1 (Applied Biosystems) and ~5 μL of each Alexa-labeled fragmented aRNA pool. Following hybridization at 45°C for 16 to 18 h, slides were washed before spin drying. Slide scanning was accomplished using an Axon 4000B scanner (Molecular Devices) using the 532- and 635-nm laser channels and a resolution of 10 μm/pixel. Data (median foreground – median background) were imported into GeneSpring GX10 for analysis using Sub-Grid LOWESS normalization (Smyth and Speed, 2003), and spots representing low signal intensity (<80) were filtered out of the analysis. Gene annotations were updated for TAIR9 and BIN annotations were added from the MapMan Site of Analysis (Thimm et al., 2004). Normalized log2 values were used to identify significant genes using a modified *t* test with SAM in Microsoft Excel (Tusher et al., 2001). An FDR of 0.05 (q-value of 5) was used as a cutoff for SAM (i.e., five genes out of 100 could be expected to be incorrectly associated as significantly changed). SAM gene lists were imported back into GeneSpring to identify DEGs with a fold change ≥1.5. Additional analyses of DEG lists included the use of Athena (O'Connor et al., 2005) to identify enriched promoter elements within 1000 bp and P values < 10^{-5} and GO terms with P values < 10^{-3}.

For *RAB18*:*ENYami* microarray analysis, Agilent Technologies *Arabidopsis* 4x44k arrays (version 4) and Low Input Quick Amp Labeling Kit (Agilent Technologies) were used. The protocol followed that detailed by the manufacturer. Two hundred nanograms of total RNA was chosen as starting material for subsequent cDNA production, and the cRNA amplification reaction proceeded for 2.5 h. Two micrograms each of cyanine 3- and 5-labeled amplified cRNA was hybridized to each array. Following washing with Agilent stabilization and drying solution, arrays were scanned individually using an Axon 4000B scanner with a resolution of 5 μm/pixel. Data analysis followed the same protocol detailed above.

Comparisons to Red Light, Quadruple *pif*, and *ga1-3* Microarray Data Sets

Microarray data comparing (1) Col-0 seed treated with either an FR light pulse or FR/R light pulses and imbibed for 12 in the dark [Col-0(R) vs Col-0 (D)] (Oh et al., 2009), (2) Col-0 seed compared with *pifq* seed after 5 d of moist chilling [*pifq*(seed) versus Col-0(seed)] (Leivar et al., 2009), and (3) *ga1-3* seed treated with 5 μM GA_4 to *ga1-3* treated with water after 9 h white light imbibition [*ga1-3*(GA)/*ga1-3*(water)] (Ogawa et al., 2003; Goda et al., 2008) were downloaded from the GEO (Barrett et al., 2009) as Affymetrix CEL files (GEO accessions GSE14374, GSE17159, and GSE5701, respectively). CEL files were inputted into GeneSpring GX10 using the GCRMA algorithm and performing the Baseline to Median of All Samples adjustment. Following Oh et al. (2009), probes with low signal intensities (<64) were filtered out of the analysis. Normalized log2 expression values were used for SAM. SAM gene lists were imported back into GeneSpring to identify DEGs with a fold change ≥1.5. DEGs from *RAB18*:*ENY* 1-h imbibed seed arrays were imported into GeneSpring and compared with the DEGs in the Col-0(D) versus Col-0(R) and Col-0(seed) versus *pifq*(seed) data sets. For comparison of *RAB18*:*ENY* and *RAB18*:*ENYami* DEGs to red light and *ga1-3* microarray data, low-signal-filtered data were exported into a new GeneSpring experiment and expressed as a log2 ratio [i.e., ratios of Col-0(R)/Col-0(D) and *ga1-3*(GA)/*ga1-3*(water)]. *RAB18*:*ENY* and *RAB18*:*ENYami* DEGs were imported and compared using a scatterplot in GeneSpring. Final data were plotted in SigmaPlot 9 (Systat Software).

Extraction and Quantification of ABA

Following lyophilization for 3 d, seeds were extractedm and ABA and dihydrophaseic acid were quantitated by the method described by Kong et al. (2008). The hormone profiling analysis was performed by HPLC-electrospray tandem mass spectrometry using deuterated internal standards by the hormone profiling service at the Plant Biotechnology Institute.

Yeast Two-Hybrid Analysis

Protein–protein interaction analysis was performed using the Matchmaker Gold yeast two-hybrid system (Clontech). The ORF of *ENY* was cloned into bait vectors pGBKT7 and pGBT9 using the In-Fusion Advantage PCR cloning kit (Clontech). Testing for autoactivation and toxicity of ENY followed the manufacturer's instructions. ENY-pGBT9, previously transformed into the Y2H Gold yeast strain, was used to screen a commercially available Mate and Plate Library (Clontech). This library was constructed from normalized *Arabidopsis* cDNA from several tissue sources, including pollen, open and closed flowers, seedlings, etiolated seedlings, siliques with seeds (3 to ~10 DPA), leaves before and after bolting, and stems. Following a 24-h mating, library screening was performed on SD/-Leu/-Trp/-His/-Ade medium with 78 ng/mL Aureobasidin A (Clontech) and 20 μg/mL x-α-Gal (Gold Biotechnology) (QDO/X/A). Following 4 d of growth at 30°C, blue yeast colonies with appreciable growth were streaked onto fresh QDO/X/A and grown for a further 3 d. Yeast plasmids were extracted using the Easy Yeast Plasmid Isolation Kit (Clontech), and cDNA inserts were PCR amplified and sequenced from the T7 promoter. The ORFs of RGA, GAI, RGL1, RGL2, and RGL3 were PCR cloned from cDNA made from seed, seedling, or flower RNA into the prey vector pGADT7 using the In-Fusion cloning kit (Clontech). For yeast mating, ENY-pGBT9 was again transformed into Y2H Gold, and each DELLA-pGADT7 was transformed into the Y187 yeast strain using the Yeastmaker Yeast Transformation System 2 (Clontech).

For quantitative assays, Y2H Gold/Y187 diploids containing ENY-pGBT9 and each DELLA-pGADT7 were used for measurements of LacZ expression and β-galatosidase activity. The liquid culture assay followed the method detailed in the Yeast Protocols Handbook (PT3024-1; Clontech) and used chlorophenol red-β-D-galactopyranoside (Roche) as a substrate. Data were compiled in Microsoft Excel and plotted using SigmaPlot 9.

BiFC

BiFC vectors, pEarleygate 100-YN and pEarleygate 100-YC, were the kind gift of Qing Lu and Yuhai Cui (Agriculture and Agri-Food Canada). These vectors were based on pEarleygate 100 (Earley et al., 2006) and were modified as described by Lu et al. (2010) except that an *Xho*I site was used to clone the N terminus (amino acids 1 to 174) and C terminus (amino acids 175 to 239) of eYFP into pEarleygate 100 ahead of the attR1 site. This creates a YFP_{1-174} or $YFP_{175-239}$ N-terminal fusion to a Gateway-cloned insert. The ORF for GAI, RGL1, RGL2, and RGL3 were cloned into pDONR221 (Life Technologies). The ORF for RGA was obtained from the ABRC in pENTR223 (Yamada et al., 2003). pEarleygate 100-YN-ENY or pEarleygate 100-YC-DELLA plasmids were transformed into *Agrobacterium*.

For infiltration into leaf epidermal cells of *Nicotiana benthamiana*, a modified version of (Schütze et al., 2009) was used. A 5-mL overnight *Agrobacterium* culture was centrifuged at 1000*g* for 10 min, resuspended in 10 mL AS medium (10 mM MES-KOH, pH 5.6, 10 mM $MgCl_2$, and 150 μM acetosyringon; prepared from stock solutions), and let to stand for 2 to 3 h. Cells containing the appropriate BiFC vectors (pEarleygate 100-YN and pEarleygate 100-YC) were brought to an OD_{600} of 0.8 to 1.0 in a 1:1:1 ratio with the tomato (*Solanum lycopersicum*) p19 plasmid (Voinnet et al., 2003). Three days after infiltration, the abaxial epidermal cells were viewed under a Zeiss LSM 510 Confor2 using the Plan-Neofluar 25X lens. eYFP images were captured using an argon 514-nm excitation, a HFT 458/514-nm major beamsplitter, 514-nm dichroic beam splitter (DBS2), a 530- to 600-nm band-pass filter, a pinhole of 500 μm, and a detector gain of ~600.

Analysis of *2x35S:ENY* Flowers and Siliques

For in vivo staining of pollen tubes, pistils from Stage 12-14 flowers (Smyth et al., 1990) were fixed overnight in 90% ethanol and 1% acetic acid. Following rinsing in a graded ethanol series (to 50%) for 20 min each, seeds were allowed to clear in Hoyer's solution for 2 h. Pistils were then treated with 1 M NaOH for 3 h before staining with decolorized analine blue overnight. Pistils were then briefly rinsed with 0.1 M K_2HPO_4 (pH 11 with KOH) and mounted on a microscope slide with 33% glycerol and 0.1 M K_2HPO_4. Images were captured using a Leica DFC320 digital camera on a Leitz Orthoplan microscope with a 4',6-diamidino-2-phenylindole filter set.

Full-length siliques were removed from three to five plants of Columbia wild type and *2x35S*:*ENY* lines. Siliques were arranged and numbered on a white piece of paper with a centimeter ruler, and photographs were taken with a tripod-mounted Canon Powershot G10 digital camera. Silique length was measured using ImageJ. Each plant line had at least 60 individual silique measurements. Following capture with the Powershot G10, siliques were dissected and seeds within each silique were counted. Data were compiled in Microsoft Excel and plotted using SigmaPlot 9.

Oil Analysis

The fatty acid profiles of 10 mg seed from Columbia wild type and *2x35S*:*ENY* lines were determined by gas chromatography using 17:0 fatty acid methyl ester as an internal standard as described by Taylor et al. (1991), Katavic et al. (1995), and Zheng et al. (2003). Data were compiled in Microsoft Excel and plotted using SigmaPlot 9.

Protein Measurement

For total protein measurements, seed was harvested from two independently grown groups of ~90 plants, and seed protein was measured with two technical replicates. Proteins were extracted from 25 mg mature seed of Columbia wild type and *2x35S*:*ENY* lines with 1 mL of 50 mM Tris-HCl, pH 8.8, 6 M Urea, 1% SDS, and 5 mM DTT. Samples were ground with ceramic spheres (Q-Biogene) in 2-mL screw cap microcentrifuge tubes with a Fast Prep FP120 machine (Q-Biogene). Following a 25-min incubation at room temp, samples were spun at 16,000*g* for 10 min at 4°C. The pellet was reextracted sequentially with 0.5 and 0.25 mL of extraction buffer. Protein in the combined supernatants was quantitated using the RC-DC protein assay (Bio-Rad) using 2 mg/mL BSA (Bio-Rad) as a standard. Data were complied in Microsoft Excel and plotted using SigmaPlot 9.

Sugar Analyses

The method for sugar extraction followed that described by Bock et al. (2009) but was modified for extraction from *Arabidopsis* and for starch. Pyrex (16 mm) tubes were rinsed twice with dichloromethane, air dried, and baked to remove any oil residue. One hundred milligrams of mature *Arabidopsis* seed from Columbia wild type and *2x35S*:*ENY* lines was ground in 2 mL 2:1 dichloromethane/isopropanol with an Omni Mixer Homogenizer (Omni International). The samples were spun at 1250*g* for 5 min, and the supernatant was removed and the pellet rinsed again with 2:1 dichloromethane/isopropanol. The pellet was dried under a gentle nitrogen stream for 2 to 3 min. The pellet was resuspended in 1 mL 80%

ethanol for 30 min with periodic vortexing (lactose was added at this step as a recovery standard). The samples were spun at 1250*g*, and the supernatant was removed to 2-mL microcentrifuge tubes. The pellet was rinsed with 0.5 mL and the supernatants combined. The samples (~1.5 mL) were dried on a speed-vac for 1 to 2 h, and samples were resuspended in 250 μL water by vortexing for 10 min. The samples were filtered through a 0.45-μm hydrophilic polypropylene membrane (GH Polypro Acrodisc; Pall Life Sciences) before adding to a HPLC vial.

The pellet from above was used to extract starch. The pellet was baked at 50°C for 30 min before adding 200 μL 0.5 M NaOH and 200 μL water and baking at 70°C for 1 h. The reaction was equilibrated with 200 μL 0.5 M HCl, allowed to cool, and 400 μL 0.2 M NaOAc, pH 4.8, was added. Two units, dissolved in 0.2 M NaOAc, of amyloglucosidase (Fluka) was added to the 1-mL suspension and mixed gently. After overnight digestion at 37°C, the reaction was stopped by heating for 10 min at 100°C. After spinning for 5 min at 1250*g*, the supernatant was transferred to a 2-mL tube, spun for 3 min at 20,000*g*, and filtered through a 0.45-μm hydrophilic polypropylene membrane (GH Polypro Acrodisc; Pall Life Sciences) before adding 250 μL to an HPLC vial.

The sugar analysis with a Dionex Bio-LC system was performed as described by Bock et al. (2009). Data were compiled in Microsoft Excel and plotted using SigmaPlot 9.

Germination Assays

Following seed sterilization, triplicates of 50 seeds were plated in 9-cm Petri dishes with two layers of 7-cm Whatman #1 Filter Paper (Fisher Scientific) with 2 mL of water and left under fluorescent white light for 1 h. Seeds were treated with 4 μmol/m^2/s FR light for 6 min or 4 μmol/m^2/s FR light for 6 min and 30 μmol/m^2/s R light for 10 min using a SNAP-LITE lighting system with 670- and 735-nm LED arrays (Quantum Devices). Seed germination was scored after 4 d in the dark. A seed was deemed germinated if the radicle had visibly protruded through the seed coat.

Germination on exogenous ABA followed Cutler et al. (2000).

Accession Numbers

Sequence data from this article can be found in the Arabidopsis Genome Initiative or GenBank/EMBL databases under the following accession numbers: IDD1/ENY (AT5G66730), ABI1 (AT4G26080), ACT2 (AT3G18780), AGF1 (AT4G35390), ALC (AT5G67110), ATHB2 (AT4G16780), BAS1 (AT2G26710), BR6OX2 (AT3G30180), COP10/FUS9 (AT3G13550), DOGT1 (AT2G36800), EXPA1 (AT1G69530), FUS3 (AT3G26790), GA2 (AT1G79460), GA3 (AT5G25900),GA2OX1 (AT1G78440), GA20OX2 (AT5G51810), GA20OX3/YAP169 (AT5G07200), GA2OX6 (AT1G02400), GA3OX1/GA4 (AT1G15550), GA3OX2/GA4H (AT1G80340), GAI (AT1G14920), GID1A (AT3G05120), GIB1B (AT3G63010), GNC (AT5G56860), IDD3/MAG (AT1G03840), IDD8/NUC (AT5G44160), IDD10/JKD (AT5G03150), IDD15/SGR5 (AT2G01940), JAZ1 (AT1G19180), LAF3 (AT3G55850), PYL11 (AT5G45860), PHYA (AT1G09570), RAB18 (AT5G66400), RGA (AT2G01570), RGL1 (AT1G66350), RGL2 (AT3G03450), RGL3 (AT5G17490), SCL3 (AT1G50420), SCR (AT3G54220), SHR (AT4G37650), SLY1 (AT4G24210), SOB7 (AT1G17060), SPA3 (AT3G15354), UBC21/PEX4 (AT5G25760), UBQ11 (AT4G05050), tobacco RSG (BAA97100), and rice YABBY1 (AF098752).

Supplemental Data

The following materials are available in the online version of this article.

Supplemental Figure 1. Defective Mucilage Extrusion in *ENY* Misexpressing Lines.

Supplemental Figure 2. Cation Chelation Promotes Mucilage Release in *ENY* Misexpressing Lines.

Supplemental Figure 3. Anther Dehiscence Is Delayed and Inhibited in *ENY-ME* Lines.

Supplemental Figure 4. Seed Production Is Lower in *ENY-ME* Lines Due to the Pollination Defect.

Supplemental Figure 5. Seeds in Siliques during Development of *ENY-ME* lines and Columbia Wild Type.

Supplemental Figure 6. Mature Embryos of *ENY-ME* Lines Were Morphologically Similar to Columbia Wild Type but Were More Translucent in Appearance.

Supplemental Figure 7. Storage Product Synthesis and Partitioning Are Disrupted in *ENY-ME* Lines.

Supplemental Figure 8. Mucilage Extrusion in *RAB18*:*ENY* Transgenic Lines Is Similar to Columbia Wild Type.

Supplemental Figure 9. Induction of *ENY* Expression in *ENY* Transgenic Lines Driven by the *RAB18* Promoter.

Supplemental Figure 10. Validation of Microarray Results.

Supplemental Figure 11. Growth of *ENY* Misexpression Seedlings under Gibberellin Treatment Results in a Skotomorphogenic-Like Phenotype.

Supplemental Figure 12. Hypocotyl Lengths of *RAB18*:*ENY* Lines 2 and 13 5 d Seedlings under ABA and GA Treatment.

Supplemental Figure 13. Expression of *ENY* in *RAB18* Overexpressing and Knockdown Lines.

Supplemental Figure 14. ENY Promotes Germination during Far-Red and Red Light Treatments.

Supplemental Figure 15. Germination of *ENY* Misexpressing Lines with and without Various Durations of Moist Chilling.

Supplemental Figure 16. ABA Sensitivity of *ENY* Transgenic Lines during Germination.

Supplemental Figure 17. Interaction of ENY and DELLA Proteins.

Supplemental Figure 18. Nuclear Localization of YFP-ENY.

Supplemental Table 1. Expression of Genes Associated with Hormonal or Light Signaling in Imbibed Seeds of *RAB18*:*ENY* and *RAB18*:*ENYami* Transgenic Lines.

Supplemental Table 2. List of PCR Primers Used in This Study.

Supplemental Data Set 1. Differentially Expressed Genes from 5 and 10 Days Postanthesis and Mature Seeds of *ENY-ME* Seed Compared with Columbia Wild Type.

Supplemental Data Set 2. Differentially Expressed Genes from *RAB18*:*ENY* Induction Experiment with Abscisic Acid.

Supplemental Data Set 3. Differentially Expressed Genes from *RAB18*:*ENY* Imbibed Seeds.

Supplemental Data Set 4. Differentially Expressed Genes from *RAB18*:*ENYami* 1 h Imbibed Seeds.

ACKNOWLEDGMENTS

We appreciate the comments and helpful suggestions from the anonymous reviewers. We thank Detlef Weigel (Salk Institute, San Diego, CA) for the amiRNA vector pRS300 and Qing Lu (Plant Biotechnology Institute) and Yuhai Cui (Agriculture and AgriFood Canada, London, Ontario, Canada) for providing the BiFC vectors. We thank the following individuals at the Plant Biotechnology Institute for discussions, suggestions, and help with experiments or data analysis: Sue Abrams, Cheryl

Bock, Fawzy Georges, Joan Krochko, Guosheng Liu, Ken Nelson, Masrur Jaradat, Ivor Smith, Tim Squires, Prakash Venglat, Liping Wang, Irina Zaharia, and Jitao Zou. We also thank Tamara Western (McGill University, Montreal, Quebec, Canada) for discussions related to mucilage extrusion. This project was supported by funding from the National Research Council of Canada through the Genomics and Health Initiative. This article is National Research Council Canada number 50169.

Received March 15, 2011; revised March 15, 2011; accepted April 25, 2011; published May 13, 2011.

REFERENCES

Abràmoff, M.D., Magalhães, P.J., and Ram, S.J. (2004). Image processing with imageJ. Biophotonics Int. **11:** 36–41.

Achard, P., Liao, L., Jiang, C., Desnos, T., Bartlett, J., Fu, X., and Harberd, N.P. (2007). DELLAs contribute to plant photomorphogenesis. Plant Physiol. **143:** 1163–1172.

Alabadí, D., Gil, J., Blázquez, M.A., and García-Martínez, J.L. (2004). Gibberellins repress photomorphogenesis in darkness. Plant Physiol. **134:** 1050–1057.

Al-Sady, B., Ni, W., Kircher, S., Schäfer, E., and Quail, P.H. (2006). Photoactivated phytochrome induces rapid PIF3 phosphorylation prior to proteasome-mediated degradation. Mol. Cell **23:** 439–446.

Angelovici, R., Galili, G., Fernie, A.R., and Fait, A. (2010). Seed desiccation: A bridge between maturation and germination. Trends Plant Sci. **15:** 211–218.

Ariizumi, T., Lawrence, P.K., and Steber, C.M. (2011). The role of two f-box proteins, SLEEPY1 and SNEEZY, in *Arabidopsis* gibberellin signaling. Plant Physiol. **155:** 765–775.

Arnaud, N., Girin, T., Sorefan, K., Fuentes, S., Wood, T.A., Lawrenson, T., Sablowski, R., and Østergaard, L. (2010). Gibberellins control fruit patterning in *Arabidopsis thaliana.* Genes Dev. **24:** 2127–2132.

Arsovski, A.A., Villota, M.M., Rowland, O., Subramaniam, R., and Western, T.L. (2009). *MUM ENHANCERS* are important for seed coat mucilage production and mucilage secretory cell differentiation in *Arabidopsis thaliana.* J. Exp. Bot. **60:** 2601–2612.

Barrett, T., et al. (2009). NCBI GEO: Archive for high-throughput functional genomic data. Nucleic Acids Res. **37**(Database issue): D885–D890.

Bewley, J.D., and Black, M. (1994). Seeds: Physiology of Development and Germination, 2nd ed. New York: Plenum Publishing).

Bock, C., Ray, H., and Georges, F. (2009). Down-regulation of galactinol synthesis in oilseed *Brassica napus* leads to significant reduction of antinutritional oligosaccharides. Botany **87:** 597–603.

Cadman, C.S.C., Toorop, P.E., Hilhorst, H.W.M., and Finch-Savage, W.E. (2006). Gene expression profiles of *Arabidopsis* Cvi seeds during dormancy cycling indicate a common underlying dormancy control mechanism. Plant J. **46:** 805–822.

Carrera, E., Holman, T., Medhurst, A., Peer, W., Schmuths, H., Footitt, S., Theodoulou, F.L., and Holdsworth, M.J. (2007). Gene expression profiling reveals defined functions of the ATP-binding cassette transporter COMATOSE late in phase II of germination. Plant Physiol. **143:** 1669–1679.

Clough, S.J., and Bent, A.F. (1998). Floral dip: a simplified method for Agrobacterium-mediated transformation of *Arabidopsis thaliana.* Plant J. **16:** 735–743.

Colasanti, J., Tremblay, R., Wong, A.Y., Coneva, V., Kozaki, A., and Mable, B.K. (2006). The *maize INDETERMINATE1* flowering time regulator defines a highly conserved zinc finger protein family in higher plants. BMC Genomics **7:** 158.

Colasanti, J., Yuan, Z., and Sundaresan, V. (1998). The indeterminate gene encodes a zinc finger protein and regulates a leaf-generated signal required for the transition to flowering in maize. Cell **93:** 593–603.

Cowling, R.J., Kamiya, Y., Seto, H., and Harberd, N.P. (1998). Gibberellin dose-response regulation of *GA4* gene transcript levels in *Arabidopsis.* Plant Physiol. **117:** 1195–1203.

Cui, H., Levesque, M.P., Vernoux, T., Jung, J.W., Paquette, A.J., Gallagher, K.L., Wang, J.Y., Blilou, I., Scheres, B., and Benfey, P.N. (2007). An evolutionarily conserved mechanism delimiting SHR movement defines a single layer of endodermis in plants. Science **316:** 421–425.

Curaba, J., Moritz, T., Blervaque, R., Parcy, F., Raz, V., Herzog, M., and Vachon, G. (2004). *AtGA3ox2*, a key gene responsible for bioactive gibberellin biosynthesis, is regulated during embryogenesis by *LEAFY COTYLEDON2* and *FUSCA3* in *Arabidopsis.* Plant Physiol. **136:** 3660–3669.

Curtis, M.D., and Grossniklaus, U. (2003). A gateway cloning vector set for high-throughput functional analysis of genes *in planta.* Plant Physiol. **133:** 462–469.

Czechowski, T., Stitt, M., Altmann, T., Udvardi, M.K., and Scheible, W.R. (2005). Genome-wide identification and testing of superior reference genes for transcript normalization in *Arabidopsis.* Plant Physiol. **139:** 5–17.

Cutler, A.J., Rose, P.A., Squires, T.M., Loewen, M.K., Shaw, A.C., Quail, J.W., Krochko, J.E., and Abrams, S.R. (2000). Inhibitors of abscisic acid 8′-hydroxylase. Biochemistry **39:** 13614–13624.

Dai, M., Zhao, Y., Ma, Q., Hu, Y., Hedden, P., Zhang, Q., and Zhou, D.X. (2007). The rice YABBY1 gene is involved in the feedback regulation of gibberellin metabolism. Plant Physiol. **144:** 121–133.

Debeaujon, I., and Koornneef, M. (2000). Gibberellin requirement for *Arabidopsis* seed germination is determined both by testa characteristics and embryonic abscisic acid. Plant Physiol. **122:** 415–424.

de Lucas, M., Davière, J.-M., Rodríguez-Falcón, M., Pontin, M., Iglesias-Pedraz, J.M., Lorrain, S., Fankhauser, C., Blázquez, M.A., Titarenko, E., and Prat, S. (2008). A molecular framework for light and gibberellin control of cell elongation. Nature **451:** 480–484.

Earley, K.W., Haag, J.R., Pontes, O., Opper, K., Juehne, T., Song, K., and Pikaard, C.S. (2006). Gateway-compatible vectors for plant functional genomics and proteomics. Plant J. **45:** 616–629.

Fei, H., Tsang, E., and Cutler, A.J. (2007). Gene expression during seed maturation in *Brassica napus* in relation to the induction of secondary dormancy. Genomics **89:** 419–428.

Feng, S., et al. (2008). Coordinated regulation of *Arabidopsis thaliana* development by light and gibberellins. Nature **451:** 475–479.

Feurtado, J.A., and Kermode, A.R. (2007). A merging of paths: Abscisic acid and hormonal cross-talk in the control of seed dormancy maintenance and alleviation. In Seed Development, Dormancy and Germination, K.J. Bradford and H. Nonogaki, eds (Oxford, UK: Blackwell Publishing), pp. 176–223.

Finkelstein, R., Reeves, W., Ariizumi, T., and Steber, C. (2008). Molecular aspects of seed dormancy. Annu. Rev. Plant Biol. **59:** 387–415.

Focks, N., and Benning, C. (1998). *wrinkled1*: A novel, low-seed-oil mutant of *Arabidopsis* with a deficiency in the seed-specific regulation of carbohydrate metabolism. Plant Physiol. **118:** 91–101.

Fujii, H., Chinnusamy, V., Rodrigues, A., Rubio, S., Antoni, R., Park, S.Y., Cutler, S.R., Sheen, J., Rodriguez, P.L., and Zhu, J.K. (2009). *In vitro* reconstitution of an abscisic acid signalling pathway. Nature **462:** 660–664.

Fukazawa, J., Nakata, M., Ito, T., Yamaguchi, S., and Takahashi, Y. (2010). The transcription factor RSG regulates negative feedback of *NtGA20ox1* encoding GA 20-oxidase. Plant J. **62:** 1035–1045.

Gazzarrini, S., Tsuchiya, Y., Lumba, S., Okamoto, M., and McCourt, P. (2004). The transcription factor *FUSCA3* controls developmental

timing in *Arabidopsis* through the hormones gibberellin and abscisic acid. Dev. Cell **7:** 373–385.

Ghassemian, M., Nambara, E., Cutler, S., Kawaide, H., Kamiya, Y., and McCourt, P. (2000). Regulation of abscisic acid signaling by the ethylene response pathway in *Arabidopsis.* Plant Cell **12:** 1117–1126.

Goda, H., et al. (2008). The AtGenExpress hormone and chemical treatment data set: experimental design, data evaluation, model data analysis and data access. Plant J. **55:** 526–542.

Griffiths, J., Murase, K., Rieu, I., Zentella, R., Zhang, Z.L., Powers, S.J., Gong, F., Phillips, A.L., Hedden, P., Sun, T.P., and Thomas, S.G. (2006). Genetic characterization and functional analysis of the GID1 gibberellin receptors in *Arabidopsis.* Plant Cell **18:** 3399–3414.

Hare, P.D., Moller, S.G., Huang, L.F., and Chua, N.H. (2003). LAF3, a novel factor required for normal phytochrome A signaling. Plant Physiol. **133:** 1592–1604.

Haughn, G., and Chaudhury, A. (2005). Genetic analysis of seed coat development in *Arabidopsis.* Trends Plant Sci. **10:** 472–477.

Helliwell, C.A., Sheldon, C.C., Olive, M.R., Walker, A.R., Zeevaart, J.A.D., Peacock, W.J., and Dennis, E.S. (1998). Cloning of the *Arabidopsis ent*-kaurene oxidase gene *GA3.* Proc. Natl. Acad. Sci. USA **95:** 9019–9024.

Heo, J.O., Chang, K.S., Kim, I.A., Lee, M.H., Lee, S.A., Song, S.K., Lee, M.M., and Lim, J. (2011). Funneling of gibberellin signaling by the GRAS transcription regulator scarecrow-like 3 in the *Arabidopsis* root. Proc. Natl. Acad. Sci. USA **108:** 2166–2171.

Holdsworth, M.J., Bentsink, L., and Soppe, W.J.J. (2008). Molecular networks regulating *Arabidopsis* seed maturation, after-ripening, dormancy and germination. New Phytol. **179:** 33–54.

Hou, X., Lee, L.Y.C., Xia, K., Yan, Y., and Yu, H. (2010). DELLAs modulate jasmonate signaling via competitive binding to JAZs. Dev. Cell **19:** 884–894.

Huang, D., Jaradat, M.R., Wu, W., Ambrose, S.J., Ross, A.R., Abrams, S.R., and Cutler, A.J. (2007). Structural analogs of ABA reveal novel features of ABA perception and signaling in *Arabidopsis.* Plant J. **50:** 414–428.

Kagaya, Y., Toyoshima, R., Okuda, R., Usui, H., Yamamoto, A., and Hattori, T. (2005). LEAFY COTYLEDON1 controls seed storage protein genes through its regulation of FUSCA3 and ABSCISIC ACID INSENSITIVE3. Plant Cell Physiol. **46:** 399–406.

Karssen, C.M., Brinkhorst-van der Swan, D.L.C., Breekland, A.E., and Koornneef, M. (1983). Induction of dormancy during seed development by endogenous abscisic acid: Studies on abscisic acid deficient genotypes of *Arabidopsis thaliana* (L.) Heynh. Planta **157:** 158–165.

Katavic, V., Reed, D.W., Taylor, D.C., Giblin, E.M., Barton, D.L., Zou, J., Mackenzie, S.L., Covello, P.S., and Kunst, L. (1995). Alteration of seed fatty acid composition by an ethyl methanesulfonate-induced mutation in *Arabidopsis thaliana* affecting diacylglycerol acyltransferase activity. Plant Physiol. **108:** 399–409.

Keith, K., Kraml, M., Dengler, N.G., and McCourt, P. (1994). *fusca3*: A heterochronic mutation affecting late embryo development in *Arabidopsis.* Plant Cell **6:** 589–600.

Kim, D.H., Yamaguchi, S., Lim, S., Oh, E., Park, J., Hanada, A., Kamiya, Y., and Choi, G. (2008). SOMNUS, a CCCH-type zinc finger protein in *Arabidopsis*, negatively regulates light-dependent seed germination downstream of PIL5. Plant Cell **20:** 1260–1277.

King, J.Y., et al. (2005). Pathway analysis of coronary atherosclerosis. Physiol. Genomics **23:** 103–118.

Kong, L., Abrams, S.R., Owen, S.J., Graham, H., and von Aderkas, P. (2008). Phytohormones and their metabolites during long shoot development in Douglas-fir following cone induction by gibberellin injection. Tree Physiol. **28:** 1357–1364.

Koornneef, M., Jorna, M.L., Brinkhorst-van der Swan, D.L.C., and Karssen, C.M. (1982). The isolation of abscisic acid (ABA) deficient mutants by selection of induced revertants in non-germinating gibberellin sensitive lines of *Arabidopsis thaliana* (L.) heynh. Theor. Appl. Genet. **61:** 385–393.

Laubinger, S., and Hoecker, U. (2003). The SPA1-like proteins SPA3 and SPA4 repress photomorphogenesis in the light. Plant J. **35:** 373–385.

Lee, K.P., Piskurewicz, U., Turecková, V., Strnad, M., and Lopez-Molina, L. (2010). A seed coat bedding assay shows that RGL2-dependent release of abscisic acid by the endosperm controls embryo growth in *Arabidopsis* dormant seeds. Proc. Natl. Acad. Sci. USA **107:** 19108–19113.

Lee, S., Cheng, H., King, K.E., Wang, W., He, Y., Hussain, A., Lo, J., Harberd, N.P., and Peng, J. (2002). Gibberellin regulates *Arabidopsis* seed germination via *RGL2*, a *GAI*/*RGA*-like gene whose expression is up-regulated following imbibition. Genes Dev. **16:** 646–658.

Leivar, P., Tepperman, J.M., Monte, E., Calderon, R.H., Liu, T.L., and Quail, P.H. (2009). Definition of early transcriptional circuitry involved in light-induced reversal of PIF-imposed repression of photomorphogenesis in young *Arabidopsis* seedlings. Plant Cell **21:** 3535–3553.

Levesque, M.P., Vernoux, T., Busch, W., Cui, H., Wang, J.Y., Blilou, I., Hassan, H., Nakajima, K., Matsumoto, N., Lohmann, J.U., Scheres, B., and Benfey, P.N. (2006). Whole-genome analysis of the SHORT-ROOT developmental pathway in *Arabidopsis.* PLoS Biol. **4:** e143.

Lotan, T., Ohto, M., Yee, K.M., West, M.A.L., Lo, R., Kwong, R.W., Yamagishi, K., Fischer, R.L., Goldberg, R.B., and Harada, J.J. (1998). *Arabidopsis* LEAFY COTYLEDON1 is sufficient to induce embryo development in vegetative cells. Cell **93:** 1195–1205.

Lu, Q., Tang, X., Tian, G., Wang, F., Liu, K., Nguyen, V., Kohalmi, S.E., Keller, W.A., Tsang, E.W., Harada, J.J., Rothstein, S.J., and Cui, Y. (2010). *Arabidopsis* homolog of the yeast TREX-2 mRNA export complex: Components and anchoring nucleoporin. Plant J. **61:** 259–270.

Luerssen, H., Kirik, V., Herrmann, P., and Miséra, S. (1998). FUSCA3 encodes a protein with a conserved VP1/AB13-like B3 domain which is of functional importance for the regulation of seed maturation in *Arabidopsis thaliana.* Plant J. **15:** 755–764.

Matsushita, A., Furumoto, T., Ishida, S., and Takahashi, Y. (2007). AGF1, an AT-hook protein, is necessary for the negative feedback of *AtGA3ox1* encoding GA 3-oxidase. Plant Physiol. **143:** 1152–1162.

McGinnis, K.M., Thomas, S.G., Soule, J.D., Strader, L.C., Zale, J.M., Sun, T.P., and Steber, C.M. (2003). The *Arabidopsis SLEEPY1* gene encodes a putative F-box subunit of an SCF E3 ubiquitin ligase. Plant Cell **15:** 1120–1130.

Morita, M.T., Saito, C., Nakano, A., and Tasaka, M. (2007). *endodermal-amyloplast less 1* is a novel allele of *SHORT-ROOT.* Adv. Space Res. **39:** 1127–1133.

Nakajima, M., et al. (2006). Identification and characterization of Arabidopsis gibberellin receptors. Plant J. **46:** 880–889.

Nambara, E., Naito, S., and McCourt, P. (1992). A mutant of *Arabidopsis* which is defective in seed development and storage protein accumulation is a new *abi3* allele. Plant J. **2:** 435–441.

Nylander, M., Svensson, J., Palva, E.T., and Welin, B.V. (2001). Stress-induced accumulation and tissue-specific localization of dehydrins in *Arabidopsis thaliana.* Plant Mol. Biol. **45:** 263–279.

O'Connor, T.R., Dyreson, C., and Wyrick, J.J. (2005). Athena: A resource for rapid visualization and systematic analysis of *Arabidopsis* promoter sequences. Bioinformatics **21:** 4411–4413.

Ogawa, M., Hanada, A., Yamauchi, Y., Kuwahara, A., Kamiya, Y., and Yamaguchi, S. (2003). Gibberellin biosynthesis and response during *Arabidopsis* seed germination. Plant Cell **15:** 1591–1604.

Oh, E., Kang, H., Yamaguchi, S., Park, J., Lee, D., Kamiya, Y., and

Choi, G. (2009). Genome-wide analysis of genes targeted by PHYTOCHROME INTERACTING FACTOR 3-LIKE5 during seed germination in *Arabidopsis.* Plant Cell **21:** 403–419.

Oh, E., Kim, J., Park, E., Kim, J.I., Kang, C., and Choi, G. (2004). PIL5, a phytochrome-interacting basic helix-loop-helix protein, is a key negative regulator of seed germination in *Arabidopsis thaliana.* Plant Cell **16:** 3045–3058.

Oh, E., Yamaguchi, S., Hu, J., Yusuke, J., Jung, B., Paik, I., Lee, H.S., Sun, T.P., Kamiya, Y., and Choi, G. (2007). PIL5, a phytochrome-interacting bHLH protein, regulates gibberellin responsiveness by binding directly to the *GAI* and *RGA* promoters in *Arabidopsis* seeds. Plant Cell **19:** 1192–1208.

Okamoto, M., et al. (2010). Genome-wide analysis of endogenous abscisic acid-mediated transcription in dry and imbibed seeds of *Arabidopsis* using tiling arrays. Plant J. **62:** 39–51.

Ooms, J.J.J., Leon-Kloosterziel, K.M., Bartels, D., Koornneef, M., and Karssen, C.M. (1993). Acquisition of desiccation tolerance and longevity in seeds of *Arabidopsis thaliana* (A comparative study using abscisic acid-Insensitive *abi3* mutants). Plant Physiol. **102:** 1185–1191.

Park, S.Y., et al. (2009). Abscisic acid inhibits type 2C protein phosphatases via the PYR/PYL family of START proteins. Science **324:** 1068–1071.

Penfield, S., Rylott, E.L., Gilday, A.D., Graham, S., Larson, T.R., and Graham, I.A. (2004). Reserve mobilization in the *Arabidopsis* endosperm fuels hypocotyl elongation in the dark, is independent of abscisic acid, and requires *PHOSPHOENOLPYRUVATE CARBOXYKINASE1.* Plant Cell **16:** 2705–2718.

Peng, J., Carol, P., Richards, D.E., King, K.E., Cowling, R.J., Murphy, G.P., and Harberd, N.P. (1997). The *Arabidopsis GAI* gene defines a signaling pathway that negatively regulates gibberellin responses. Genes Dev. **11:** 3194–3205.

Piskurewicz, U., Jikumaru, Y., Kinoshita, N., Nambara, E., Kamiya, Y., and Lopez-Molina, L. (2008). The gibberellic acid signaling repressor RGL2 inhibits *Arabidopsis* seed germination by stimulating abscisic acid synthesis and ABI5 activity. Plant Cell **20:** 2729–2745.

Piskurewicz, U., Turecková, V., Lacombe, E., and Lopez-Molina, L. (2009). Far-red light inhibits germination through DELLA-dependent stimulation of ABA synthesis and ABI3 activity. EMBO J. **28:** 2259–2271.

Pfaffl, M.W. (2001). A new mathematical model for relative quantification in real-time RT-PCR. Nucleic Acids Res. **29:** e45.

Phillips, J., Artsaenko, O., Fiedler, U., Horstmann, C., Mock, H.P., Müntz, K., and Conrad, U. (1997). Seed-specific immunomodulation of abscisic acid activity induces a developmental switch. EMBO J. **16:** 4489–4496.

Poppenberger, B., Fujioka, S., Soeno, K., George, G.L., Vaistij, F.E., Hiranuma, S., Seto, H., Takatsuto, S., Adam, G., Yoshida, S., and Bowles, D. (2005). The UGT73C5 of *Arabidopsis* thaliana glucosylates brassinosteroids. Proc. Natl. Acad. Sci. USA **102:** 15253–15258.

Reed, J.W., Nagatani, A., Elich, T.D., Fagan, M., and Chory, J. (1994). Phytochrome A and phytochrome B have overlapping but distinct functions in *Arabidopsis* development. Plant Physiol. **104:** 1139–1149.

Richter, R., Behringer, C., Müller, I.K., and Schwechheimer, C. (2010). The GATA-type transcription factors GNC and GNL/CGA1 repress gibberellin signaling downstream from DELLA proteins and PHYTOCHROME-INTERACTING FACTORS. Genes Dev. **24:** 2093–2104.

Santos-Mendoza, M., Dubreucq, B., Baud, S., Parcy, F., Caboche, M., and Lepiniec, L. (2008). Deciphering gene regulatory networks that control seed development and maturation in *Arabidopsis.* Plant J. **54:** 608–620.

Schütze, K., Harter, K., and Chaban, C. (2009). Bimolecular fluorescence complementation (BiFC) to study protein-protein interactions in living plant cells. In Plant Signal Transduction, T. Pfannschmidt, ed (New York: Humana Press), pp. 189–202.

Schmid, M., Davison, T.S., Henz, S.R., Pape, U.J., Demar, M., Vingron, M., Schölkopf, B., Weigel, D., and Lohmann, J.U. (2005). A gene expression map of *Arabidopsis* thaliana development. Nat. Genet. **37:** 501–506.

Schwab, R., Ossowski, S., Riester, M., Warthmann, N., and Weigel, D. (2006). Highly specific gene silencing by artificial microRNAs in *Arabidopsis.* Plant Cell **18:** 1121–1133.

Seo, P.J., Ryu, J., Kang, S.K., and Park, C.M. (2011). Modulation of sugar metabolism by an INDETERMINATE DOMAIN transcription factor contributes to photoperiodic flowering in *Arabidopsis.* Plant J. **65:** 418–429.

Shen, Y., Khanna, R., Carle, C.M., and Quail, P.H. (2007). Phytochrome induces rapid PIF5 phosphorylation and degradation in response to red-light activation. Plant Physiol. **145:** 1043–1051.

Shin, J., Kim, K., Kang, H., Zulfugarov, I.S., Bae, G., Lee, C.H., Lee, D., and Choi, G. (2009). Phytochromes promote seedling light responses by inhibiting four negatively-acting phytochrome-interacting factors. Proc. Natl. Acad. Sci. USA **106:** 7660–7665.

Shinomura, T., Nagatani, A., Chory, J., and Furuya, M. (1994). The induction of seed germination in *Arabidopsis thaliana* is regulated principally by phytochrome B and secondarily by phytochrome A. Plant Physiol. **104:** 363–371.

Silverstone, A.L., Ciampaglio, C.N., and Sun, T. (1998). The *Arabidopsis RGA* gene encodes a transcriptional regulator repressing the gibberellin signal transduction pathway. Plant Cell **10:** 155–169.

Silverstone, A.L., Tseng, T.S., Swain, S.M., Dill, A., Jeong, S.Y., Olszewski, N.E., and Sun, T.P. (2007). Functional analysis of SPINDLY in gibberellin signaling in *Arabidopsis.* Plant Physiol. **143:** 987–1000.

Singh, D.P., Jermakow, A.M., and Swain, S.M. (2002). Gibberellins are required for seed development and pollen tube growth in *Arabidopsis.* Plant Cell **14:** 3133–3147.

Smyth, D.R., Bowman, J.L., and Meyerowitz, E.M. (1990). Early flower development in *Arabidopsis.* Plant Cell **2:** 755–767.

Smyth, G.K., and Speed, T. (2003). Normalization of cDNA microarray data. Methods **31:** 265–273.

Steindler, C., Matteucci, A., Sessa, G., Weimar, T., Ohgishi, M., Aoyama, T., Morelli, G., and Ruberti, I. (1999). Shade avoidance responses are mediated by the ATHB-2 HD-zip protein, a negative regulator of gene expression. Development **126:** 4235–4245.

Stone, S.L., Kwong, L.W., Yee, K.M., Pelletier, J., Lepiniec, L., Fischer, R.L., Goldberg, R.B., and Harada, J.J. (2001). LEAFY COTYLEDON2 encodes a B3 domain transcription factor that induces embryo development. Proc. Natl. Acad. Sci. USA **98:** 11806–11811.

Strasser, B., Sánchez-Lamas, M., Yanovsky, M.J., Casal, J.J., and Cerdán, P.D. (2010). *Arabidopsis thaliana* life without phytochromes. Proc. Natl. Acad. Sci. USA **107:** 4776–4781.

Sun, T. (2008). Gibberellin metabolism, perception and signaling pathways in *Arabidopsis*. In The Arabidopsis Book **6:** e0103, doi/10.1199/tab.0103.

Suzuki, G., Yanagawa, Y., Kwok, S.F., Matsui, M., and Deng, X.W. (2002). Arabidopsis COP10 is a ubiquitin-conjugating enzyme variant that acts together with COP1 and the COP9 signalosome in repressing photomorphogenesis. Genes Dev. **16:** 554–559.

Tanimoto, M., Tremblay, R., and Colasanti, J. (2008). Altered gravitropic response, amyloplast sedimentation and circumnutation in the *Arabidopsis shoot gravitropism 5* mutant are associated with reduced starch levels. Plant Mol. Biol. **67:** 57–69.

Taylor, D.C., Weber, N., Barton, D.L., Underhill, E.W., Hogge, L.R., Weselake, R.J., and Pomeroy, M.K. (1991). Triacylglycerol bioassembly

in microspore-derived embryos of *Brassica napus* L. cv Reston. Plant Physiol. **97:** 65–79.

Thimm, O., Bläsing, O., Gibon, Y., Nagel, A., Meyer, S., Krüger, P., Selbig, J., Müller, L.A., Rhee, S.Y., and Stitt, M. (2004). MAPMAN: A user-driven tool to display genomics data sets onto diagrams of metabolic pathways and other biological processes. Plant J. **37:** 914–939.

Thomas, S.G., Phillips, A.L., and Hedden, P. (1999). Molecular cloning and functional expression of gibberellin 2- oxidases, multifunctional enzymes involved in gibberellin deactivation. Proc. Natl. Acad. Sci. USA **96:** 4698–4703.

Tiedemann, J., Rutten, T., Mönke, G., Vorwieger, A., Rolletschek, H., Meissner, D., Milkowski, C., Petereck, S., Mock, H.P., Zank, T., and Bäumlein, H. (2008). Dissection of a complex seed phenotype: novel insights of *FUSCA3* regulated developmental processes. Dev. Biol. **317:** 1–12.

To, A., Valon, C., Savino, G., Guilleminot, J., Devic, M., Giraudat, J., and Parcy, F. (2006). A network of local and redundant gene regulation governs *Arabidopsis* seed maturation. Plant Cell **18:** 1642–1651.

Turk, E.M., et al. (2005). BAS1 and SOB7 act redundantly to modulate *Arabidopsis* photomorphogenesis via unique brassinosteroid inactivation mechanisms. Plant J. **42:** 23–34.

Tusher, V.G., Tibshirani, R., and Chu, G. (2001). Significance analysis of microarrays applied to the ionizing radiation response. Proc. Natl. Acad. Sci. USA **98:** 5116–5121.

Tyler, L., Thomas, S.G., Hu, J., Dill, A., Alonso, J.M., Ecker, J.R., and Sun, T.P. (2004). Della proteins and gibberellin-regulated seed germination and floral development in *Arabidopsis.* Plant Physiol. **135:** 1008–1019.

Voinnet, O., Rivas, S., Mestre, P., and Baulcombe, D. (2003). An enhanced transient expression system in plants based on suppression of gene silencing by the p19 protein of tomato bushy stunt virus. Plant J. **33:** 949–956.

Welch, D., Hassan, H., Blilou, I., Immink, R., Heidstra, R., and Scheres, B. (2007). *Arabidopsis* JACKDAW and MAGPIE zinc finger proteins delimit asymmetric cell division and stabilize tissue boundaries by restricting SHORT-ROOT action. Genes Dev. **21:** 2196–2204.

West, M.A.L., Yee, K.M., Danao, J., Zimmerman, J.L., Fischer, R.L., Goldberg, R.B., and Harada, J.J. (1994). LEAFY COTYLEDON1 is an essential regulator of late embryogenesis and cotyledon identity in *Arabidopsis.* Plant Cell **6:** 1731–1745.

Western, T.L., Skinner, D.J., and Haughn, G.W. (2000). Differentiation of mucilage secretory cells of the *Arabidopsis* seed coat. Plant Physiol. **122:** 345–356.

White, C.N., Proebsting, W.M., Hedden, P., and Rivin, C.J. (2000). Gibberellins and seed development in maize. I. Evidence that gibberellin/abscisic acid balance governs germination versus maturation pathways. Plant Physiol. **122:** 1081–1088.

Willige, B.C., Ghosh, S., Nill, C., Zourelidou, M., Dohmann, E.M.N., Maier, A., and Schwechheimer, C. (2007). The DELLA domain of GA INSENSITIVE mediates the interaction with the GA INSENSITIVE DWARF1A gibberellin receptor of *Arabidopsis.* Plant Cell **19:** 1209–1220.

Wong, A.Y.M., and Colasanti, J. (2007). Maize floral regulator protein INDETERMINATE1 is localized to developing leaves and is not altered by light or the sink/source transition. J. Exp. Bot. **58:** 403–414.

Xu, Y.L., Li, L., Gage, D.A., and Zeevaart, J.A.D. (1999). Feedback regulation of *GA5* expression and metabolic engineering of gibberellin levels in *Arabidopsis.* Plant Cell **11:** 927–936.

Yamada, K., et al. (2003). Empirical analysis of transcriptional activity in the *Arabidopsis* genome. Science **302:** 842–846.

Yamaguchi, S., Smith, M.W., Brown, R.G.S., Kamiya, Y., and Sun, T. (1998). Phytochrome regulation and differential expression of gibberellin 3β-hydroxylase genes in germinating *Arabidopsis* seeds. Plant Cell **10:** 2115–2126.

Yoshida, T., Nishimura, N., Kitahata, N., Kuromori, T., Ito, T., Asami, T., Shinozaki, K., and Hirayama, T. (2006). *ABA-hypersensitive germination3* encodes a protein phosphatase 2C (AtPP2CA) that strongly regulates abscisic acid signaling during germination among *Arabidopsis* protein phosphatase 2Cs. Plant Physiol. **140:** 115–126.

Zentella, R., Zhang, Z.L., Park, M., Thomas, S.G., Endo, A., Murase, K., Fleet, C.M., Jikumaru, Y., Nambara, E., Kamiya, Y., and Sun, T.P. (2007). Global analysis of DELLA direct targets in early gibberellin signaling in *Arabidopsis.* Plant Cell **19:** 3037–3057.

Zhang, Z.L., Ogawa, M., Fleet, C.M., Zentella, R., Hu, J., Heo, J.O., Lim, J., Kamiya, Y., Yamaguchi, S., and Sun, T.P. (2011). Scarecrow-like 3 promotes gibberellin signaling by antagonizing master growth repressor DELLA in *Arabidopsis.* Proc. Natl. Acad. Sci. USA **108:** 2160–2165.

Zheng, Z., Xia, Q., Dauk, M., Shen, W., Selvaraj, G., and Zou, J. (2003). *Arabidopsis AtGPAT1*, a member of the membrane-bound glycerol-3-phosphate acyltransferase gene family, is essential for tapetum differentiation and male fertility. Plant Cell **15:** 1872–1887.